

Mass Movement and Landform Degradation on the Icy Galilean Satellites: Results of the Galileo Nominal Mission

Jeffrey M. Moore, Erik Asphaug, and David Morrison

NASA Ames, MS 245-3, Moffett Field, California 94035

E-mail: jmoore@ringside.arc.nasa.gov

John R. Spencer

Lowell Observatory, Flagstaff, Arizona 86001

Clark R. Chapman and Beau Bierhaus

Southwest Research Institute, 1050 Walnut Street, Suite 426, Boulder, Colorado 80302

Robert J. Sullivan, Frank C. Chuang, James E. Klemaszewski, Ronald Greeley, and Kelly C. Bender

Geology Department, Arizona State University, Tempe, Arizona 85287

Paul E. Geissler

Lunar Planetary Laboratory, University of Arizona, Tucson, Arizona 85721

Paul Helfenstein

Center for Radiophysics and Space Research, Cornell University, Ithaca, New York 14853

and

Carl B. Pilcher

NASA Headquarters, Washington, DC 20546

Received June 18, 1998; revised March 2, 1999

The Galileo mission has revealed remarkable evidence of mass movement and landform degradation on the icy Galilean satellites of Jupiter. Weakening of surface materials coupled with mass movement reduces the topographic relief of landforms by moving surface materials down-slope. Throughout the *Galileo* orbiter nominal mission we have studied all known forms of mass movement and landform degradation of the icy galilean satellites, of which Callisto, by far, displays the most degraded surface. Callisto exhibits discrete mass movements that are larger and apparently more common than seen elsewhere. Most degradation on Ganymede appears consistent with sliding or slumping, impact erosion, and regolith evolution. Sliding or slumping is also observed at very small (100 m) scale on Europa. Sputter ablation, while probably playing some role in the evolution of Ganymede's and Callisto's debris layers, appears to be less important than other processes. Sputter ablation might play a significant role on Europa only if that satellite's surface is significantly older than 10^8 years, far older than crater statistics indicate. Impact erosion and regolith formation on Europa are probably min-

imal, as implied by the low density of small craters there. Impact erosion and regolith formation may be important on the dark terrains of Ganymede, though some surfaces on this satellite may be modified by sublimation-degradation. While impact erosion and regolith formation are expected to operate with the same vigor on Callisto as on Ganymede, most of the areas examined at high resolution on Callisto have an appearance that implies that some additional process is at work, most likely sublimation-driven landform modification and mass wasting. The extent of surface degradation ascribed to sublimation on the outer two Galilean satellites implies that an ice more volatile than H_2O is probably involved. © 1999 Academic Press

Key Words: Europa; Ganymede; Callisto; satellites of Jupiter; satellite surfaces.

INTRODUCTION

Mass movement and landform degradation reduce topographic relief by moving surface materials to a lower gravitational

potential. In addition to the obvious role of gravity, abrasive mechanical erosion plays a role, often in combination with the lowering of cohesion which allows disaggregation of the relief-forming material. The identification of specific landform types associated with mass movement and landform degradation provides information about local sediment particle size and abundance and transportation processes. Generally, mass movements can be classified in terms of the particle sizes of the transported material and the speed the material moved during transport (Sharpe 1939, Varnes 1958, Coates 1977). Such schemes have been used to characterize mass movements on Mercury, Venus, the Moon, Mars, and Io (e.g., Sharp 1973a, 1973b, Malin and Dzurisin 1977, Malin 1992, Schenk and Bulmer 1998), although the character of extraterrestrial movements can only be inferred from the resulting deposits' morphologies since resolution is nearly always insufficient to observe individual particles within the deposits. Modification of slopes on icy galilean satellites (excluding impact-related crater modifications, such as terraced crater interiors) is not obvious in Voyager images. On Venus, the improvement in resolution from Venera 15/16 (~ 2 km/pixel) to Magellan (~ 150 m/pixel) was essential in the recognition and classification of mass movements (Malin 1992, Bulmer and Guest 1996). Similarly, Galileo images acquired at ≤ 100 m/pixel resolution and high incidence angle and/or in stereo were usually required to reveal landforms on these satellites characteristic of mass movement. In this study we: (1) identify landforms and surface textures that are indicative of mass movement and landform degradation; (2) develop working hypotheses for the evolution of these landforms and surface materials; and (3) model the parameters of various hypotheses which can be tested against the observations.

OBSERVATIONS AND INTERPRETATIONS

Europa

Among the icy Galilean satellites, evidence for landform degradation is least obvious on Europa. The most abundant, if not the solitary, expressions of simple downslope mass wasting on Europa are lower slope components distinguished by nearly uniform gradients and smooth texture that commonly are subjacent to more rugged and slightly steeper materials. The lower, smoother units are most likely accumulations of debris at the bases of scarps and slopes, probably at or near the angle of repose. These deposits are relatively small, usually extending < 1 km outward, and are unambiguously seen only in imaging < 30 m/pixel. A good example was observed at 21 m/pixel along the base of a ridge at $\sim 15^\circ\text{N}$, 173°W (Fig. 1). This ridge doublet stands ~ 300 m above its surroundings, and the steepest slopes on the illuminated flank are $\sim 42^\circ$ with an average gradient of $\sim 36^\circ$ (Kadel *et al.* 1998). Lower portions of this ridge flank are less steep, smoother, darker materials that drape over and partly cover older terrain as they extend outward. We interpret these lower slope units as accumulations of debris derived from materials immediately above (Fig. 1, arrow A). A bright,

more rugged, and slightly steeper scarp along the upper slopes of the ridge flank is observed above much of the darker, putative debris (Fig. 1, arrow B), in some places taking the form of chutes (Fig. 1, arrow C). Individual particles within the talus are not seen at this resolution, with the exception of three isolated 100-m-scale blocks near the base of the ridge that probably were derived from the upslope of material. These blocks are directly beneath what may be a down-glided kilometer-sized tabular slab. As the large isolated blocks appear only here, it is possible that they are associated with the putative movement of this large slab.

The few impact craters seen in Fig. 1 (exclusive of those associated with an ejecta ray from Pwyll lying across the right half of the image) are below the density of craters at the Surveyor 7 site on the rim of the lunar crater Tycho. An analysis of the Tycho-Surveyor 7 site concluded that the impact-generated regolith there was < 15 cm thick (Shoemaker and Morris 1969). Thus the amount of impact-produced regolith in the scene shown in Fig. 1 is probably insufficient to account for the quantity of loose material required to generate the talus deposits. Some other debris-producing process must be invoked to account for the observed quantities of loose material. The presence of talus at or near the angle of repose immediately subjacent to slightly steeper scarps along many European slopes implies that overall gradients have been reduced as slopes have degraded and talus has accumulated. Presumably, at the start of talus production, slope exposures steeper than the angle of repose were more extensive. Steep scarps greater than the angle of repose might have been produced by uplift due to endogenic forces (e.g., Pappalardo *et al.* 1998b) or steeply dipping fractures along plate margins (Schenk and McKinnon 1989, Golombek and Banerdt 1990).

Ganymede

Galileo images indicate more diverse styles of mass wasting on Ganymede than have been seen on Europa. This might be related to the greater range of surface ages seen on Ganymede. Mass movement on Ganymede at the smallest observable scale visible by Galileo SSI consists of numerous dark streaks on slopes (see Prockter *et al.* 1998b, Pappalardo *et al.* 1998a for further discussion and examples). These dark streaks are seen on all terrains observed at resolutions better than 100 m/pixel, although they are less prevalent on light terrains. High-resolution, stereo coverage in Uruk Sulcus and Galileo Regio confirm that dark streaks reside on steep slopes and are oriented down-gradient. Slopes with dark streaks in this stereo coverage have up to 1 km relief and gradients of about 10° . These streaks always appear superposed on other materials, implying they are superficial deposits. These streaks often widen toward the base, consistent with the idea that this material has moved downslope. Low albedo material occupying topographic lows, sometimes as broad, coalesced bases of adjacent streaks (see area left of black arrow in Fig. 2), may be further evidence of downslope movement. In several places this material appears to collect in the form of short, thick, coalescing lobes at the base of slopes; the best example is seen along the base of southeast wall

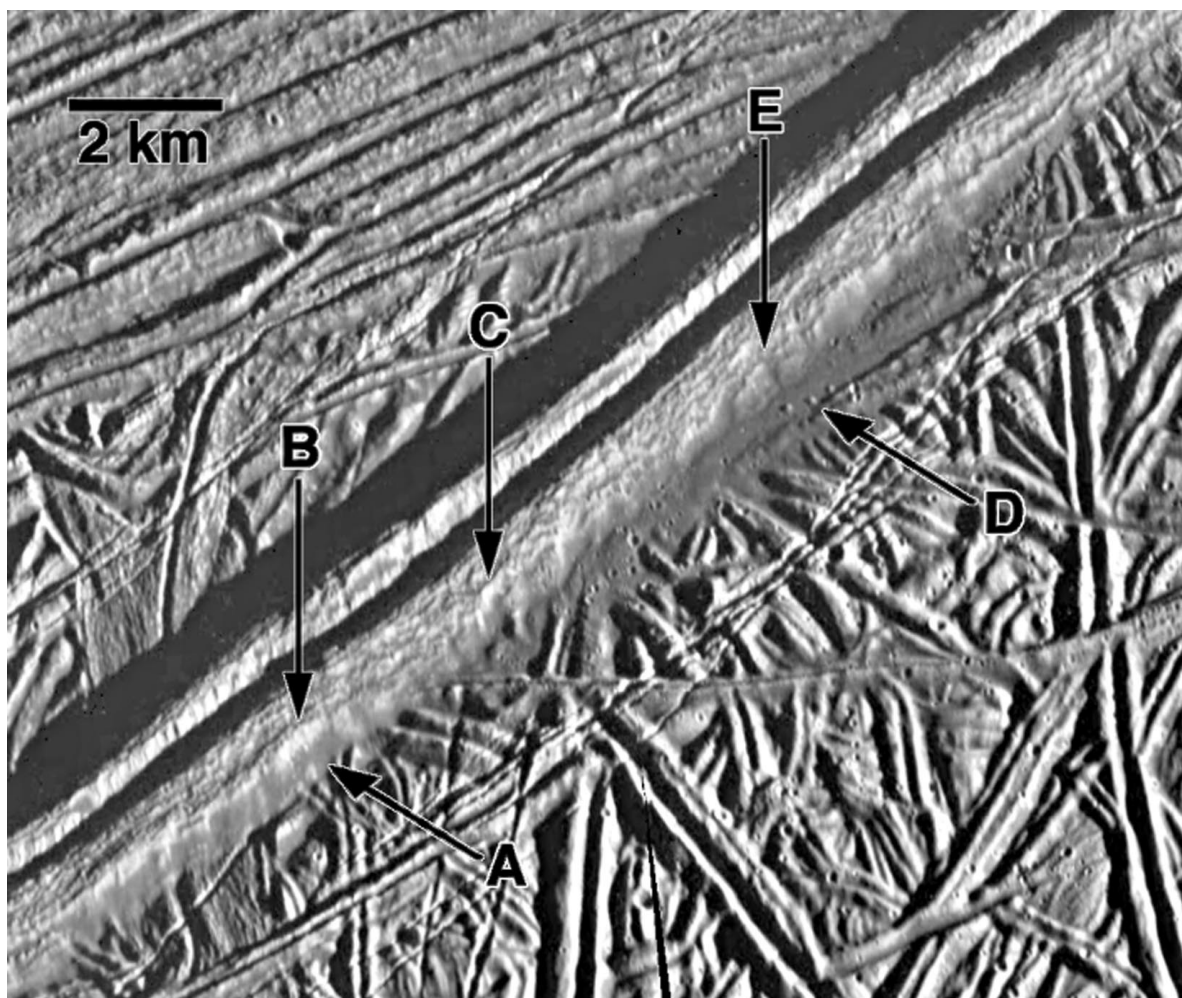


FIG. 1. High-resolution (~ 20 m/pixel), low-sun oblique-looking image of a young ridge on Europa exhibiting pattern changes interpreted to be accumulations of debris at the bases of scarps and slopes (see arrow A). A bright, steep scarp along the upper slopes of the ridge can be seen above much of the debris (arrow at B). In some places taking the form of chutes (arrow at C). Three isolated 100-m-scale blocks near the base of the ridge probably were derived from materials up-slope (arrow at D). These blocks are directly beneath what may be a down-glided kilometer-sized tabular slab (arrow at E). As the large isolated blocks appear only here, it is possible that they are associated with the putative movement of this large slab. Illumination is from the lower right. North is up. Scene center coordinates are 16°N , 173°W . (A portion of Galileo image PICNO E6E0074.)

of the crater Ea in Galileo Regio (see area beyond white arrow in Fig. 2).

Lowering of relief presumably involving slope degradation and recession has affected terrain in Nicholson Regio observed at 180 m/pixel during orbit G7. The intermediate-albedo unit (see image and sketch map in Fig. 3) is scarp-bounded in places and stands higher than surrounding darker materials. Craters on the intermediate-albedo plateau generally have more prominent raised rims than craters in the surrounding lower, darker terrain (see A in sketch map of Fig. 3). Some craters straddling the boundary between these two units have raised rims only on the brighter plateau (see B in sketch map of Fig. 3), and portions of crater rims outside the plateau in the lower, darker unit are less distinct. Relatively subdued crater rims in the darker material give the impression of shallower crater depths compared with craters on the brighter plateau (see dotted circles in sketch map

of Fig. 3). Crater floors within the darker material are sometimes even darker than other areas within this unit. We infer that the brighter plateau material has eroded by scarp retreat, leaving behind darker materials showing degraded craters with subdued rims. We consider two possibilities to explain what is observed. First, there may be a relatively simple stratigraphy of brighter materials overlying darker materials. In this scenario the brighter materials are susceptible to some form of degradation and removal, revealing the darker unit underneath. This process would occur primarily at steep slope exposures, consistent with the mostly scarp-controlled boundary of the brighter plateau we see in the images. Craters large enough to originally penetrate through the brighter unit into the underlying darker unit would, once the brighter material was stripped away, remain as shallow, subdued “ghosts” lacking distinct raised rims. However, complete removal of an overlying brighter unit is probably too

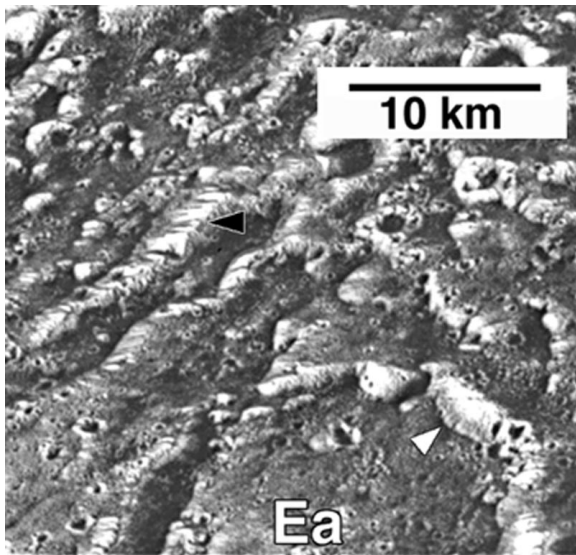


FIG. 2. Commonly seen evidence for mass movement on Ganymede consists of numerous dark streaks on slopes, as seen here in this high-sun, 70 m/pixel image of Galileo Regio. These streaks often widen toward the base of the slopes upon which they reside, suggesting a talus-like geometry and down-slope motion. Further evidence of down-slope movement of unconsolidated material is observed in low-albedo material occupying topographic lows, sometimes in the form of broad, coalesced bases of adjacent streaks (area left of black arrow). In several places this material appears to collect in the form of short, thick, coalescing lobes at the base of slopes; the best example is seen along the base of southeast wall of the crater Ea in Galileo Regio (area beyond white arrow). North is to the left. Scene center coordinates are 17.5°N, 146°W. (A portion of Galileo image PICNO G1G0023.)

simplistic. More likely, much of the original material remained behind as debris, contributing to reduced crater relief. Alternatively, a second, simpler idea involves no distinct layering. In this scenario the process of scarp recession around the margins of brighter units produces darker debris that is left behind to drape over lowered terrain, partially protecting it from further degradation. Some volume loss during scarp recession is implied in this scenario, as well, to explain the general lowering of terrain in the wake of the receding scarps. There are a few prominent-rimmed craters within the dark material, among the more abundant subdued-rimmed craters. Their paucity suggests that they probably formed after brighter scarps had retreated.

The very highest resolution (11 m/pixel, 83° incidence angle) images of Ganymede were acquired at 30°N, 90°W, during orbit G1 in an area that has recently been named Xibalba Sulci. Unfortunately, the imaged area contained unexpectedly bright slopes that were overexposed and thus saturated portions of the SSI CCD, producing pixel bleed that obscures portions of these images. Nevertheless, several possible examples of mass movement and landform modification are recognizable (Fig. 4). The best regional context available is a low incidence, 830 m/pixel image of this same region acquired during orbit C9 which indicates that the terrain sampled at 11 m/pixel-resolution has intermediate albedo, is smooth at 830 m/pixel and is super-

posed on ancient dark terrain (Fig. 5). In the regional view, this “smooth” material, where it is seen between solitary grooves which cross it at ~40-km intervals, exhibits almost no structural texture and is marred only by small impact craters and a few indeterminate bright dots (speculated to be even smaller impact craters).

At very high resolution (Fig. 4), the same surface is almost nowhere smooth. The most prominent features are N to NW oriented elongate hills commonly ≤ 1 km long and standing ~50 m above their surroundings (from shadow measurements). The largest hill is ~2 km long and ~200 m high. Hill orientation is similar to the solitary grooves seen in the C9 image, implying a tectonic origin. Slopes are usually less than ~10°, although in a few instances they approach ~20°. Slopes are commonly brighter and smoother than their surroundings.

This terrain has craters ranging in diameter from 1.5 km down to the limit of resolution. The presentation of many of the craters is different from that of similar-sized craters on the Earth’s Moon. Some craters appear partially infilled (see craters marked “C” in Fig. 4). The surface between the hills is generally undulatory with a rough texture composed of components near the limit of resolution. This surface has been aptly labeled the “goosebump plains” (Yingst *et al.* 1997), but will be referred to in this study as the “rough plains.” The rough plains unit is the most areally extensive surface seen in these images, with textures suggestive of hummocks or block or boulder clusters. A few small patches (a few hundred meters across) of smooth material overlie the rough plains, usually near the bases of hills. The rough plains sometimes abruptly terminate short of contact with a hill, forming a partial moat (see “A” in Fig. 4). Seen especially well in shadows illuminated by scattered light are “dark” streaks whose locations and organization appear controlled by the local topographic gradient (see “S” in Fig. 4). We interpret the dark streaks to be loose material that has moved down-slope. Curiously, this material also mantles hill tops in a manner that implies that it is not being derived from the hills themselves but has been superposed from above (see areas marked “M” in Fig. 4). Additional description and analysis of these images can be found in Yingst *et al.* (1997, 1998).

This area may once have been covered more extensively by rough plains material. In this scenario, some mechanism has eroded and reduced the rough plains material, exhuming stratigraphically older craters and smooth hills. Patches of this formerly extensive rough plains material still mantle the partly exhumed surface. The moats around the higher albedo hills may indicate that removal of rough plains material has been partly influenced by solar insolation. Sunlight reflected off the hills may increase the heating of immediately adjacent material causing volatiles within this material to sublimate. If this hypothesis is correct, the volatile must have been a major constituent of this unit. Such a volatile substance (both in Xibalba Sulci and in Nicholson Regio) would have to be less thermally stable than H₂O. Candidate volatiles and sublimation degradation mechanisms will be discussed later.

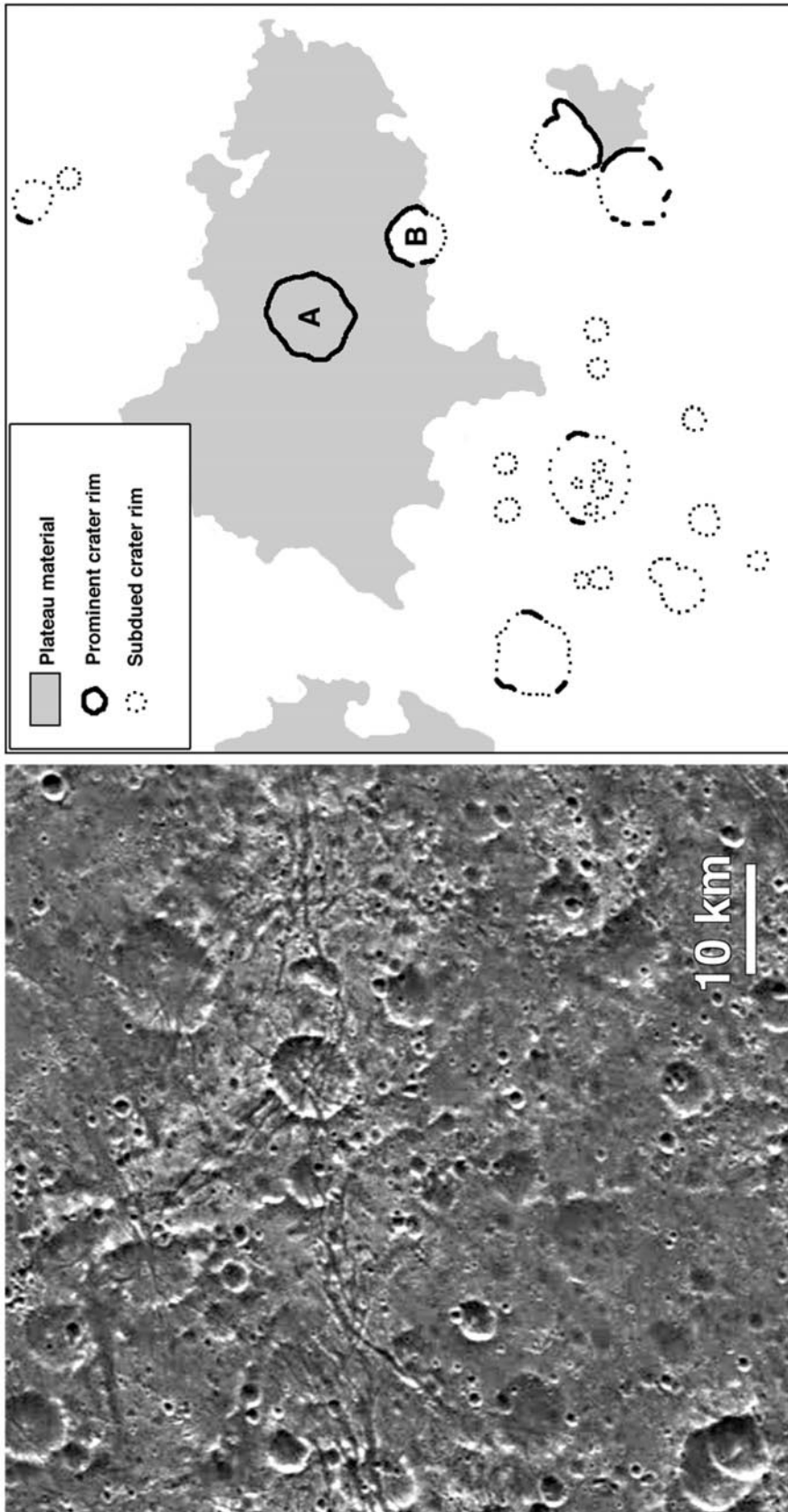


FIG. 3. A landscape in Nicholson Regio, implying that Ganymede that may exhibit large-scale mass wasting involving scarp retreat and the formation of a lag deposit. The sun is moderately low and from the right. Image resolution is 180 m/pixel. North is up. Scene center coordinates are 12.5°S, 354°W. (A portion of Galileo image PICNO G7G0010.)

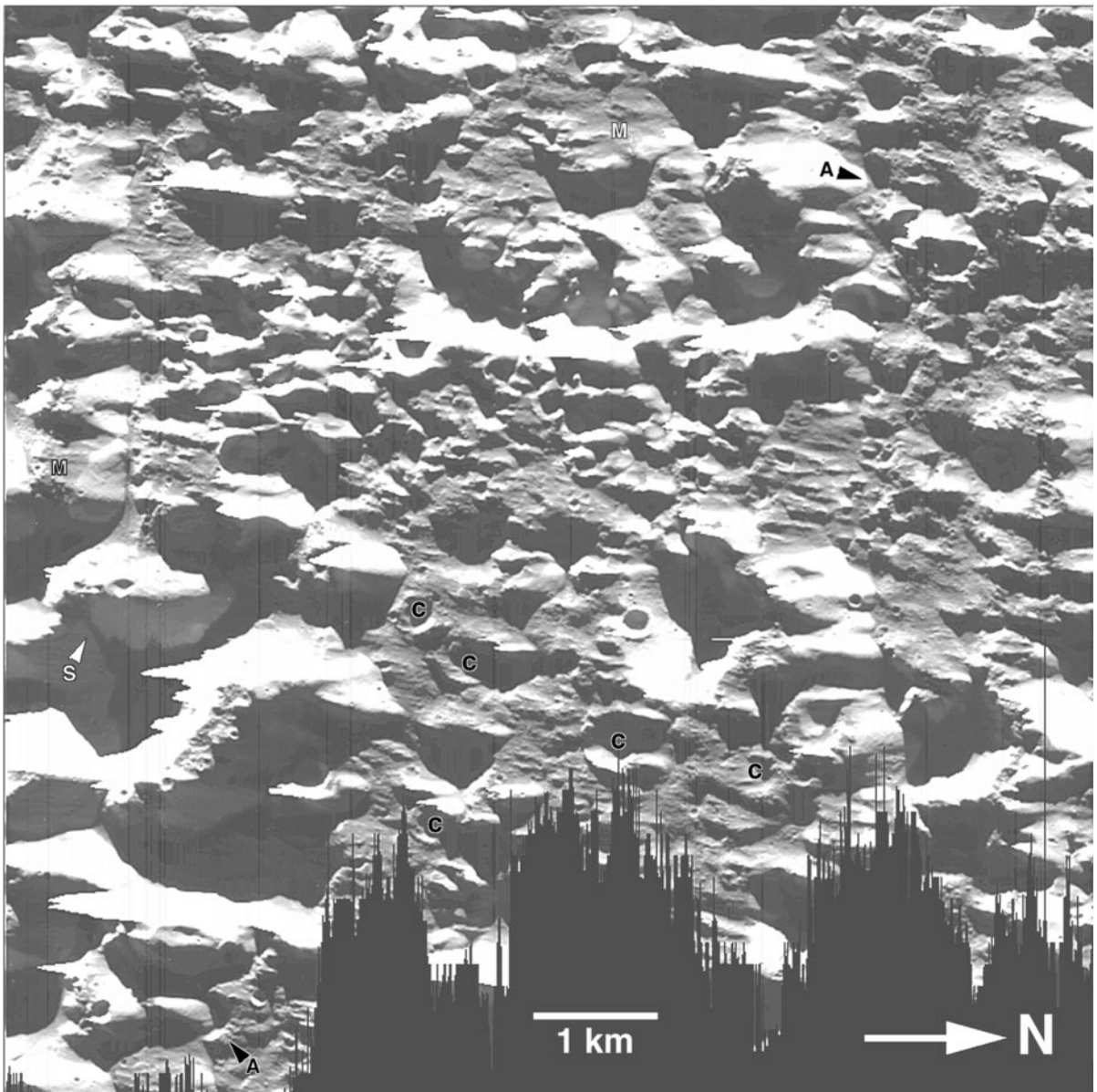


FIG. 4. A very high-resolution (11 m/pixel), low-sun image acquired of Ganymede at location 30°N , 90°W (Xibalba Sulci). Unfortunately, the imaged area contained unexpectedly bright slopes that saturated portions of the SSI CCD, producing pixel bleed which obscures portions of this image (the pixel bleed forms the bright left-pointing “icicles”). The dark lines along the bottom were caused by data truncation. Nevertheless, enough detail can be seen that possible examples of mass movement and landform modification are recognizable. The dark lines along the bottom were caused by data truncation. See text for details. (Galileo image PICNO G1G0043.)

Callisto

Kilometer-scale craters on Ganymede’s dark terrain observed at <100 m/pixel (Fig. 6) show a range of morphologies, which are, to first order, characteristic of modification by the subsequent rain of mostly smaller impacts (Prockter *et al.* 1998b). In contrast, the kilometer-scale craters on Callisto seen by Galileo at <60 m/pixel range from those with continuous, sharp-crested bright rims and bowl-like interior topography to craters whose raised rims have become very discontinuous and whose interiors have become shallower (Fig. 7). The material composing the

rims appears to disaggregate in a manner that resembles decomposition of the rim-forming bedrock itself rather than pulverization by small impacts. The disaggregated dark material may be a by-product of rim-forming bedrock disintegration. (Relatively small differences between the appearances of fresh craters in Figs. 6 and 7 may be due to variable amounts of rim frost between the two targets. Resolution and lighting differences between the two original data sets may also contribute to these dissimilarities.)

Moreover, 100-m to kilometer-scale craters on Callisto are underabundant relative to Ganymede dark terrain though both

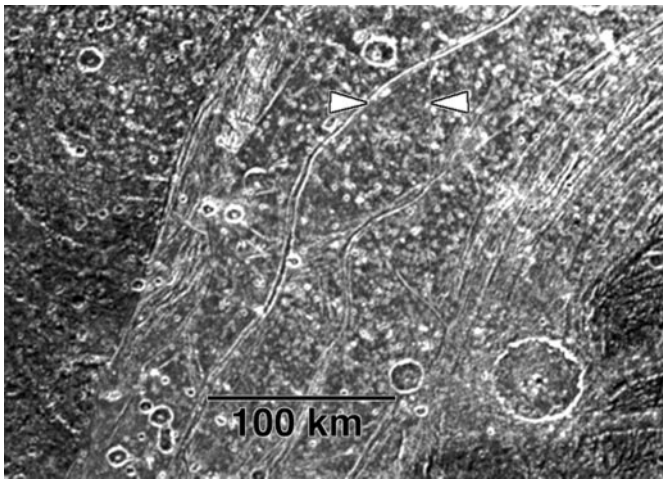


FIG. 5. A high-sun, 830 m/pixel image of the region shown in Fig. 4 shows an intermediate-albedo, smooth (at 830 m/pixel) deposit that appears younger and superposed on ancient dark terrain. The arrows indicate a candidate site for the imaging acquired at high resolution. In the regional view, this “smooth” material, where it is seen between solitary grooves which cross it at ~ 40 -km intervals, exhibits almost no structural texture and is marred only by small impact craters and a few indeterminate bright dots. North is up. (A portion of Galileo image PICNO C9G0002.)

terrains are thought to be approximately the same age (e.g., McKinnon and Parmentier 1986). As can be seen in Fig. 8, the level or dipping-to-the-left trends for Ganymede and Callisto, respectively, represent unusually “shallow” size-frequency trends (i.e., differential power-law indices in the range of -1.5 to -3) for craters of these sizes, compared with crater populations on such bodies as the Moon and Gaspra. This drop off may partly reflect a relative dearth of small comets impacting in the Jupiter system (Chapman *et al.* 1998). But the *difference* between

Ganymede and Callisto (i.e., the much shallower slope for all units of Callisto examined at high resolution) reflects strongly size-dependent crater destruction on Callisto, since the production function for impactors striking Ganymede and Callisto must be the same. We associate size-dependent crater loss with the disaggregation process, which liberates materials that evidently fill in crater floors beneath their crumbling ramparts.

To first order, Callisto’s surface is either bright (geometric albedo $A = \sim 0.8$) or dark ($A = \sim 0.2$) with very little variation in between. Bright material probably is frost (e.g., Spencer 1987a). Bright material often occurs near or at the crests of high standing topography, such as crater rims. If bright material is frost, then these frost deposits may be relatively thin (not greater than a few meters). The putative frost coatings do not appear to have changed, muted, or exaggerated the topography or shape of these outcrops at Galileo resolutions. For instance, the bright rims of the craters in Fig. 7 do not stand higher above surrounding terrain (as determined from shadow measurements) than rims of similar-sized and similarly preserved craters on the Earth’s Moon (Pike 1980). Large expanses of bright surfaces appear texturally rough; have steep, inconstant slopes; and exhibit an overall appearance of an otherwise unmantled bedrock (Fig. 9). Bright frost may preferentially form on bedrock, which will have a higher thermal inertia and hence remain colder throughout the day.

In contrast, the dark material is almost always present in low-lying areas or in plains away from any relief. On scarps, it sometimes forms a smooth-textured lower component with a constant gradient (see between black arrows in Fig. 9). The contact of the dark material with the rugged and steeper upper slope forms fan-like upward-pointing V’s, implying that dark material was derived from up-slope, perhaps down chutes (see slopes below white arrow in Fig. 9). The derived thermal inertia for this

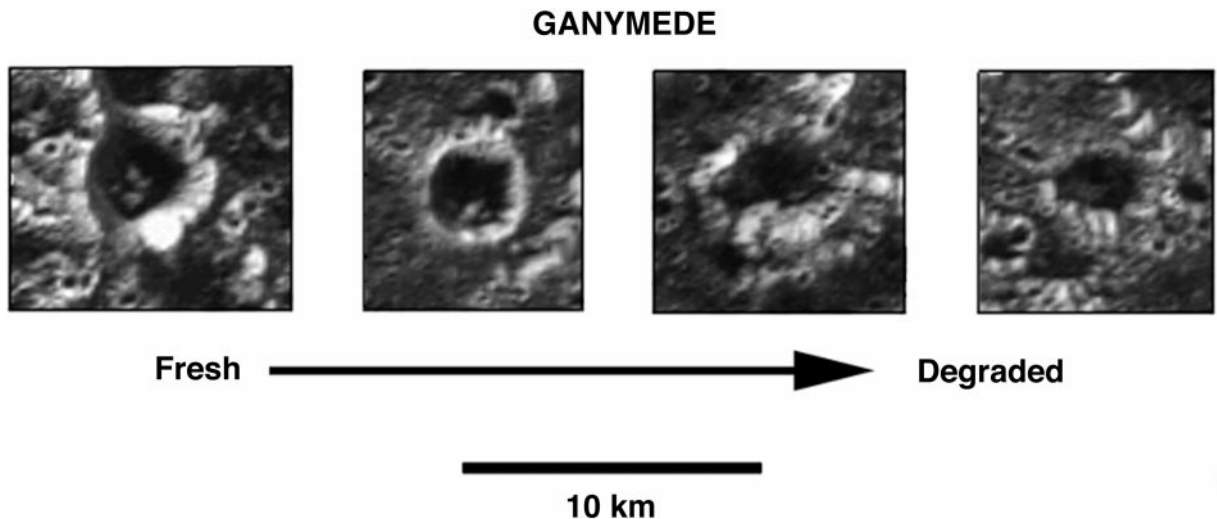


FIG. 6. Kilometer-scale craters on Ganymede’s dark terrain show a range of morphologies, which are generally characteristic of modification by the subsequent rain of mostly smaller impacts. These examples were all taken from high-sun, 70 m/pixel images of Galileo Regio. North is up. Examples are located near $\sim 18^\circ\text{N}$, 149°W . (Excerpted from Galileo images PICNO G1G0021, 22, 23, 24.)

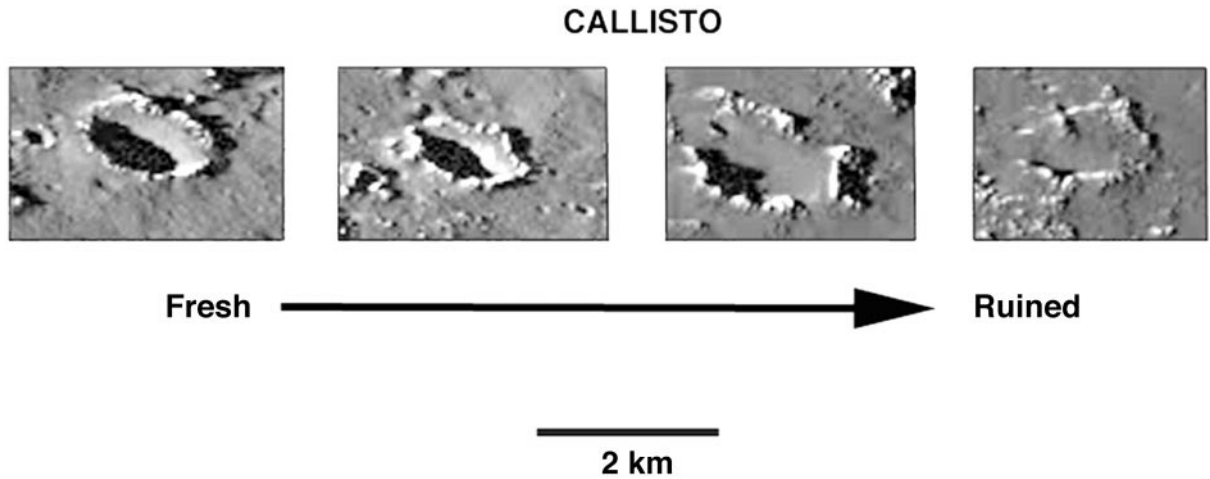


FIG. 7. Kilometer-scale craters on Callisto range from those with more-or-less continuous, sharp-crested bright rims and bowl-like interior topography to craters with discontinuous rims and shallow interiors. The rim material appears to disaggregate in a manner that resembles decomposition of the rim-forming bedrock itself rather than pulverization by small impacts. The loose fine-grained dark material may be a by-product of rim-forming bedrock disintegration. These examples were all taken from low-sun, 50 m/pixel oblique-looking images. Illumination is from the left. The left two examples are located near $\sim 38^\circ\text{N}$, 35°W ; the right two examples are located near $\sim 35^\circ\text{N}$, 46°W . (Excerpted from Galileo images PICNO C3C0044, 45, 65, 66.)

material is $< 5 \times 10^4 \text{ erg cm}^{-2} \text{ s}^{-0.5} \text{ K}^{-1}$ (Spencer 1987b), implying that it is composed of unconsolidated micrometer-sized particles. Dark material commonly appears smooth even in the highest resolution images ($\sim 35 \text{ m/pixel}$). Smooth patches of dark material approaching 5 km across can be seen within crater floors or in intercrater depressions (Fig. 10). The absence of topography within the smooth patches may indicate that the dark material may be many meters thick here. Dark material may fall on Callisto from external sources, such as interplanetary dust or material derived from Jupiter's small outer satellites (see review by McKinnon and Parmentier 1986). However, regional color variations of dark material on Callisto observed by Galileo (Denk *et al.* 1998) suggest a crustal source for this material, rather than an exotic origin from beyond the satellite. A crustal origin is consistent with the visual impression of dark material being derived locally from bedrock-supported landforms, such as crater rims.

Kilometer-scale degradation and mass movements on Callisto have several manifestations. The most commonly seen expression of discrete mass movement is slumps or slides, sometimes accompanied by lateral spreading of the fallen material, which will be referred to collectively as debris aprons (Figs. 11 and 12). Debris aprons on Callisto are found in several different observations representing a latitude range of $\sim 35^\circ\text{N}$ to 5°S and two different longitudes ($\sim 0^\circ\text{W}$ and $\sim 145^\circ\text{W}$). Debris aprons are observed most often within craters, with putative slide detachment on the inner rim and debris deposits on the floor. Five debris aprons were observed well enough to derive good morphometry. The heights from which the debris aprons originate range from ~ 0.5 to almost 1 km. The deposits from any one slide form a solitary lobe with runout lengths from 1.7 to 4.4 km and areas from ~ 3 to $\sim 11 \times 10^6 \text{ m}^2$. Lobes range from semicircular to tongue-like and have smooth surfaces and lack digitate edges;

the edges have steep terminations ($\sim 20^\circ$). Lobes appear to be of nearly constant thickness (50–100 m) out to their edges. Debris aprons are nearly uniformly dark, although some exhibit slight albedo variation, but without an obvious organized pattern. No longitudinal or transverse textures are obvious on the surfaces of the debris deposits at the available resolution (88 and 160 m/pixel). Terrestrial and extraterrestrial aprons with these characteristics have been interpreted to be debris avalanches (e.g., Sharpe 1939, Sharp 1973b, Malin 1992). On this basis, we interpret the aprons in Figs. 11 and 12 to be debris avalanches. Additional discussion of Callistan debris aprons can be found in Chuang *et al.* (1998).

In order to compare Callistan mass movements with those elsewhere in the solar system, we plotted several parameters of these features (non-Callistan data from Bulmer 1994, Schenk and Bulmer 1998). Comparing height versus length ratio (H/L) with slide volume shows that Callistan debris aprons are generally smaller and were less energetic than most mass movements from the Moon, Mars, or Io (Fig. 13a). Callistan debris aprons are similar to the smaller martian aprons. McEwen (1989) suggested that martian landslide emplacement has half the runout efficiency of Earth, and the same may be true on Callisto. Perhaps this inefficiency is caused by the gravitational effects on the yield strength of materials with Bingham rheology (McEwen 1989) or lack of a lubricating inter-pore liquid or dense atmospheric gas (e.g., Brunsten 1979, p. 142). Alternatively, the apparent relative inefficiency may be due to differences in the type and amount of available loose material (e.g., Varnes 1958). In Fig. 13b, H/L is plotted against runout distance, now including data from escarpments on Venus (Malin 1992) as well. Callistan debris aprons plot among the shorter runout terrestrial subaerial mass movements, despite their nonterrestrial inefficiency as illustrated in Fig. 13a. Such short runout distances may account

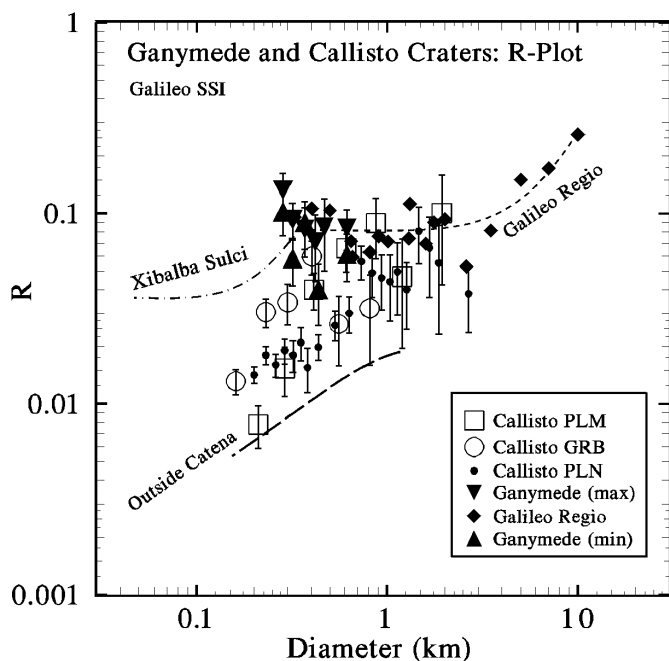


FIG. 8. Plot of relative crater densities on selected cratered terrains of Ganymede and Callisto illustrates different trends on the two satellites. The surfaces of Callisto and on Ganymede’s dark terrain are thought to be ancient (~ 4 Gyr old), yet the paucity of 100-m-scale craters on Callisto relative to Ganymede is obvious. Crater counts for Callisto were taken from the low-sun, 35-to-50 m/pixel “Palimpsest” (PLM), “Graben” (GRB), and “Plains” (PLN) image sequences acquired during the C3 orbit. Trends for small craters on Callisto [including the fit for counts (individual points not shown) for small craters outside of the large catena craters in the Gipul catena sequence] trend upward toward the right at a slope of $1/2$ to 1 , whereas counts for Ganymede are nearly horizontal or sloping upward only slightly. Diamonds without error bars and associated line fit for Galileo Regio are shown, as well as a fit to counts of very small craters on Xibalba Sulci (observed at 11 m/pixel) which represent the minimum crater densities counted on Ganymede. “Max” and “min” indicate the range of best estimates of crater densities just outside of Memphis Facula, studied from the overlapping region of two moderately high-resolution frames. (“min” indicates craters independently identified on both of the frames; “max” indicates craters identified on one or the other of the frames.) The nearly horizontal (differential power-law index = -3) slope for Ganymede at smaller diameters is shallower than the typical -4 to -4.5 slope for inner solar system crater curves at these sizes, suggesting a relative depletion of smaller impactors. But the -2 to -2.5 slope for Callisto implies an additional factor, presumably related to the disaggregation and filling processes on the undulating smooth units on Callisto.

for the characteristic thickness and lobate margins of Callistan aprons.

Aprons of material lie adjacent to and, in some cases, apparently overlap each other in the floors of some large craters. In the example shown in Fig. 12, these lobate aprons extend ~ 10 km from the inner crater wall. The walls above the aprons appear steeper than elsewhere along the walls where sheets are not seen. If these aprons are debris avalanche deposits, then they are thinner and exhibit more irregular edges than the examples shown in Fig. 11. Perhaps these features indicate that material composing

debris avalanche deposits is subject to further modification and degradation. If these aprons are debris avalanche deposits, then in some instances avalanches have contributed significantly to crater enlargement through scarp retreat.

Three of the four debris avalanches seen in an image transect of the Asgard region originate along the east wall of their parent craters, and the fourth originates from a southeast wall (Fig. 11). All may have formed simultaneously in response to a large distant impact-induced seismic event. Others, such as the debris avalanche seen in Fig. 14 (labeled “S”), may have been triggered by local impacts. Debris avalanches of the sizes seen on Callisto have not been found on the other icy Galilean satellites. Thus, either the processes responsible for slope destabilization on Callisto are more effective or the nature of the surface layer is different on this satellite. One possibility is that the mechanical integrity of Callisto’s bedrock may be dependent upon interstitial volatile ice. In this case, local topography-controlled variations in insolation would control sublimation loss of volatile ice within the bedrock. This hypothesis will be explored in the discussion section.

A 375 by 225-km region at 1°S , 6°W , displays several landforms probably indicative of landscape modification through mass movement (Fig. 14). In addition to the debris apron noted earlier, this landscape contains a number of pits, which often occur in clusters. These pits are sharply outlined, closed depressions with steep walls but no raised outer rims. Outlines range from simple and smoothly curving to complexly convoluted but rarely angular. Some pits appear to have formed by coalescence or are barely separated from one another by septa. Large pits are deeper than small pits. From shadow measurements, the largest pits have depths approaching 1 km. The pits have a monomodal planimetric size distribution with a peak around 1 km but skewed toward the smaller members (Merline *et al.* 1998). Pit configuration and morphology are inconsistent with a secondary impact origin, so if they were initially formed by secondaries, they have been greatly modified. These pits resemble the martian polar etched pits first described by Sharp (1973a), and they may have a similar origin. Callistan pits may have formed from initially unremarkable local depressions by the differential sublimation of a volumetrically substantial volatile in which the shape of the growing pit acted to concentrate solar energy into the pits’ centers, this process becoming more efficient with increasing size. An equatorial location allows direct sunlight into even deep pits. The uneven distribution of pits and pit clusters may reflect a heterogeneous distribution of the putative subsurface volatile. The role and composition of volatiles will be discussed in the next section.

Several crater walls are gullied with radial valley-like incisions in north or northeast facing crater walls (Fig. 14). Individual “gullies” at this location are <500 m wide and <4 km long. Gullies extend from rim crests down to crater floor level. Many other craters in the same scene show subtler radial patterns on portions of their walls. Since erosion by fluid drainage and downcutting is unlikely, an alternative possibility is that the

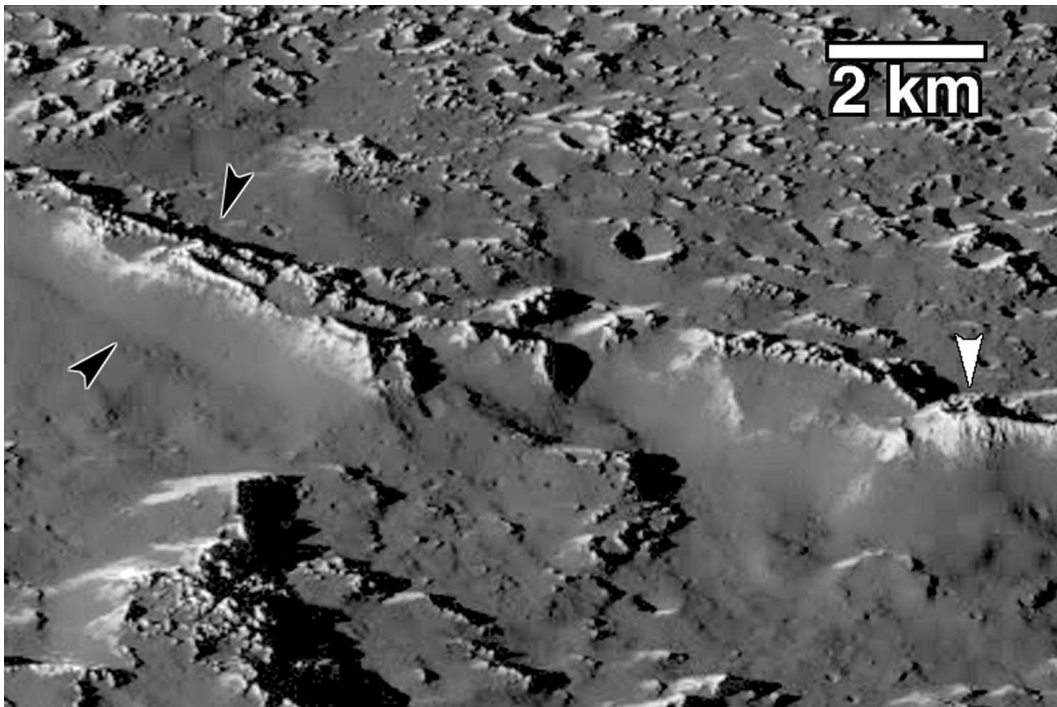


FIG. 9. Bright and dark material on Callisto's surface seen at low sun and high resolution. If bright material is frost, then these deposits may be relatively thin (not greater than a few meters). Large expanses of bright surfaces, such as the scarp seen here, appear texturally rough, have steep inconstant slopes, and exhibit the overall appearance of an otherwise unmantled bedrock. Bright frost may preferentially form on bedrock, which will have a higher thermal inertia and hence remain colder throughout the day. In contrast, the dark material at the base of scarps sometimes forms a smooth-textured lower component of constant-angle slope, as can be seen at the base of the scarp in the left side of the figure (see slopes between black arrows). The contact of the lower dark material with the rugged and steeper upper slope may trace out upward-pointing "V"s, implying that dark material has moved from up-slope, perhaps down-chutes (see slopes below white arrow). Oblique-looking, 40 m/pixel resolution image of a portion of the southern wall of Gomul Catena at 35°N, 46°W. Illumination is from the lower right. (A portion of Galileo image PICNO C3C0046.)

same process that formed the pits and predisposed the formation of debris avalanches is widening preexisting fractures in and beyond the crater walls. The original radial fractures could have formed as part of the cratering process. Recent images of Ganymede's dark terrain acquired during orbits G7 and G8 show fractures and graben converging on craters in a fashion consistent with an exploitation of impact-induced radial lines of weakness by postimpact regional extensional stress (e.g., Asphaug *et al.* 1998, Prockter *et al.* 1998a).

DISCUSSION

The icy Galilean satellites show clear and unambiguous evidence of mass movements at a variety of scales and probably employing a variety of mechanisms. We now consider what may be producing these different landforms and surface textures. Mass wasting on much of Ganymede and along locally steep slopes on Europa appears consistent, to first order, with "dry" movements. Debris aprons attributed to debris avalanches on Callisto also probably move in a dry mode. These dry movements appear to involve rock and debris, where gravity and oversteepened slopes were major prerequisites. Here the term dry is being applied using a popular terrestrial mass movement

classification (e.g., see Coates 1977, Malin 1992, his Fig. 2) that plots material cohesion and particle size against speed of movement. This scheme groups mass movements requiring fluidizing lubrication (whether from air or water) to one extreme and those which require no lubricant (and hence dry) at the other. On the icy Galilean satellites, sputtering, impact-derived regolith production, and sublimation probably all play roles in the evolution and redistribution of their surficial layers. We will next discuss these mechanisms in detail.

Sputtering

The potential effect of sputtering decreases substantially with increasing distance from Jupiter. Hence, Europa should be most affected by this process. Malin and Pieri (1986) reviewed post-Voyager work examining the role of sputtering in ground ablation, noting that several studies, based on essentially the same type of modeling, derive a considerable range of ablation rates (450 to 0.50 m/Gyr), making it difficult to evaluate the true potential of sputtering as a geomorphic agent. New results from the energetic particle detector on the Galileo orbiter were used to estimate a net sputtering ablation rate of roughly 200 m/Gyr (Ip *et al.* 1998). If the age of Europa's landscape is on the

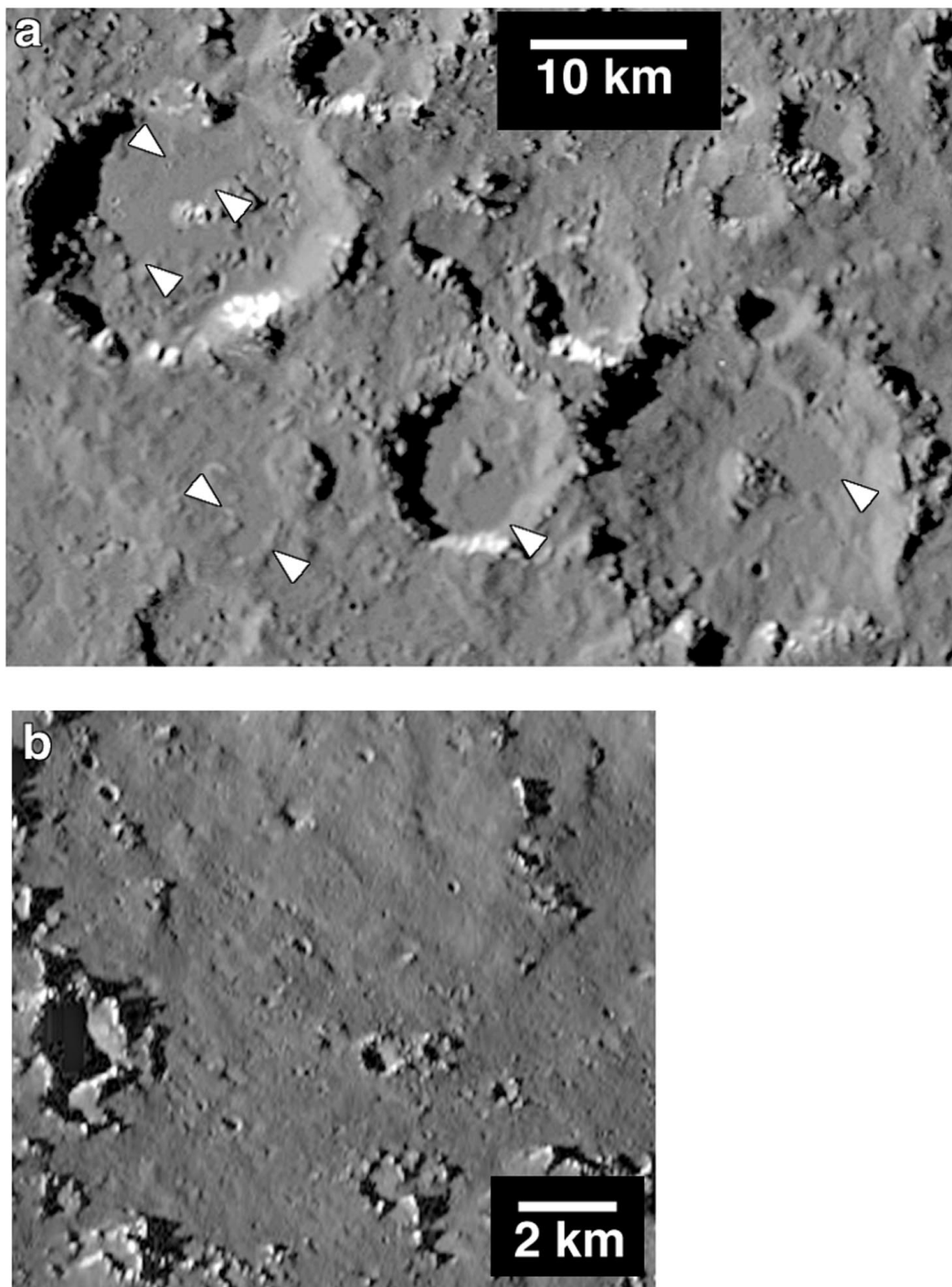


FIG. 10. (a). Smooth patches (see arrows) of dark material on Callisto, approaching 5 km across, can be seen within crater floors or in intercrater depressions of this low-sun, 160 m/pixel image. The absence of topography within the smooth patches implies that the dark material may be locally many meters thick. Scene center coordinates are $\sim 38^{\circ}\text{N}$, 35°W . (A portion of Galileo image PICNO C9C0010.) (b) Dark material commonly appears smooth even in the highest resolution images. This low-sun (incidence angle $\sim 85^{\circ}$), 37 m/pixel image shows a few several-hundred-meter-scale craters. Scene center coordinates are $\sim 8^{\circ}\text{S}$, 7°W . In both images north is up and illumination is from the west. (A portion of Galileo image PICNO C3C0066 in orthographic projection.)

order of 10^7 years, and not greater than 10^8 years as Zahnle *et al.* (1998) and Chapman *et al.* (1998) suggest, then sputtering could only be playing a role detectable at Galileo imaging resolutions (≥ 6 m/pixel) if the highest estimates for sputtering ablation are correct.

The effectiveness of sputtering on ice is 20 times less at Ganymede and 100 times less at Callisto than at Europa (Johnson 1990). The recently discovered significant magnetic field of Ganymede (Kivelson *et al.* 1996) may further shield that satellite from the effects of sputtering. Shoemaker *et al.* (1982) pointed

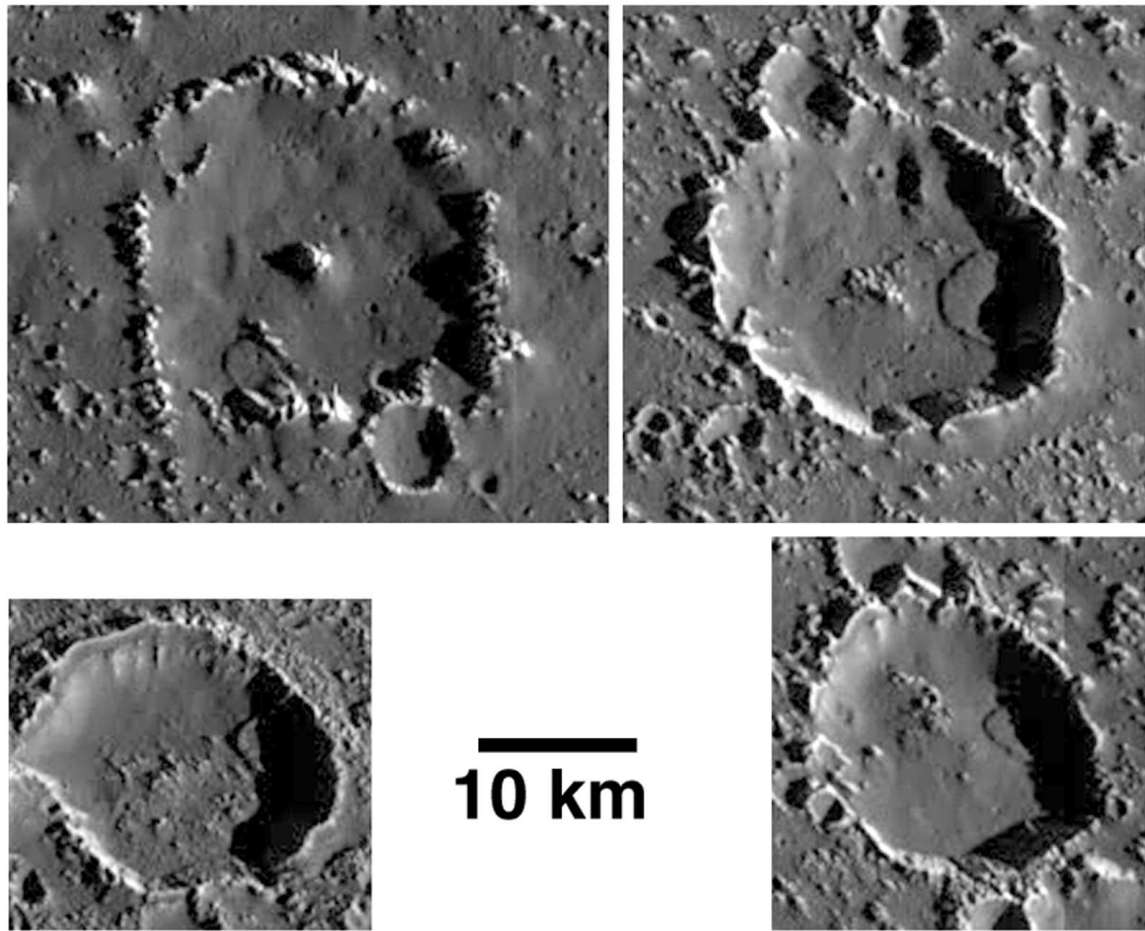


FIG. 11. Debris aprons interpreted to be debris avalanches in craters of the Asgard region, Callisto. All examples are taken from low-sun, 88 m/pixel images. North is up and illumination is from the east. See text for detailed analysis. Examples are taken from a north-south image transect along the $\sim 149^\circ\text{W}$ longitude and between the latitudes of $\sim 18^\circ\text{N}$ and $\sim 27^\circ\text{N}$. (Excerpted from Galileo images PICNO C10C0003, 04, 09.)

out that the ice-rich crater rays on Ganymede, which Passey and Shoemaker (1982) calculate have a probable survival age of ~ 1 Gyr, are probably not more than a few meters thick and so may be taken as an indicator that ice sputter-*ablation* rate on this satellite may be low (i.e., less than a few meters per gigayear). Passey and Shoemaker (1982) derive a similar probable Callistan crater ray retention age with the same implication for ice sputter-*ablation* rates. Prockter *et al.* (1998b) point out that the presence of a north/south-facing slope dichotomy in surface frosts on the dark terrain of Ganymede implies that the rate of sublimation-driven thermal ice segregation (as proposed by Spencer 1987a) is not greater than the sputtering rate. The contribution of sputter *ablation*, while it may play a role in the evolution of Ganymede's and Callisto's debris layers, appears to be of secondary importance.

Impact Cratering and Regolith Generation

As was stated under Observations and Interpretations, Europa appears sufficiently uncratered that the effects of impact-produced regolith would not be seen in Galileo imaging. Prockter

et al. (1998b) reported that one of the most striking aspects of the appearance of the dark terrain on Ganymede (where seen at < 100 m/pixel) is that the topography appears "softened" at small scales when compared to younger grooved terrain, particularly in the rounded crests of furrows and crater rims (Figs. 2 and 6). They attributed this softening to micrometeorite bombardment and suggested that the resulting morphologies may be comparable with those seen on the lunar highlands (assuming that the microimpactor flux was at least roughly equivalent to that of the Moon). Though there is reason to suspect that the number of primary impactors capable of making craters less than a few kilometers in diameter are less abundant in the jovian system than has been the case for the Moon (e.g., Chapman *et al.* 1998), the density of small, subkilometer-scale craters on Galileo Regio imply that there has been time for saturation-equilibrium crater densities to develop on this surface, presumably with a significantly higher relative contribution from secondaries than on the Moon.

High-resolution images of Callisto reveal a pervasive covering by a smooth, slightly undulating unit of generally homogeneous low albedo and texture (Fig. 10), originally revealed in imaging

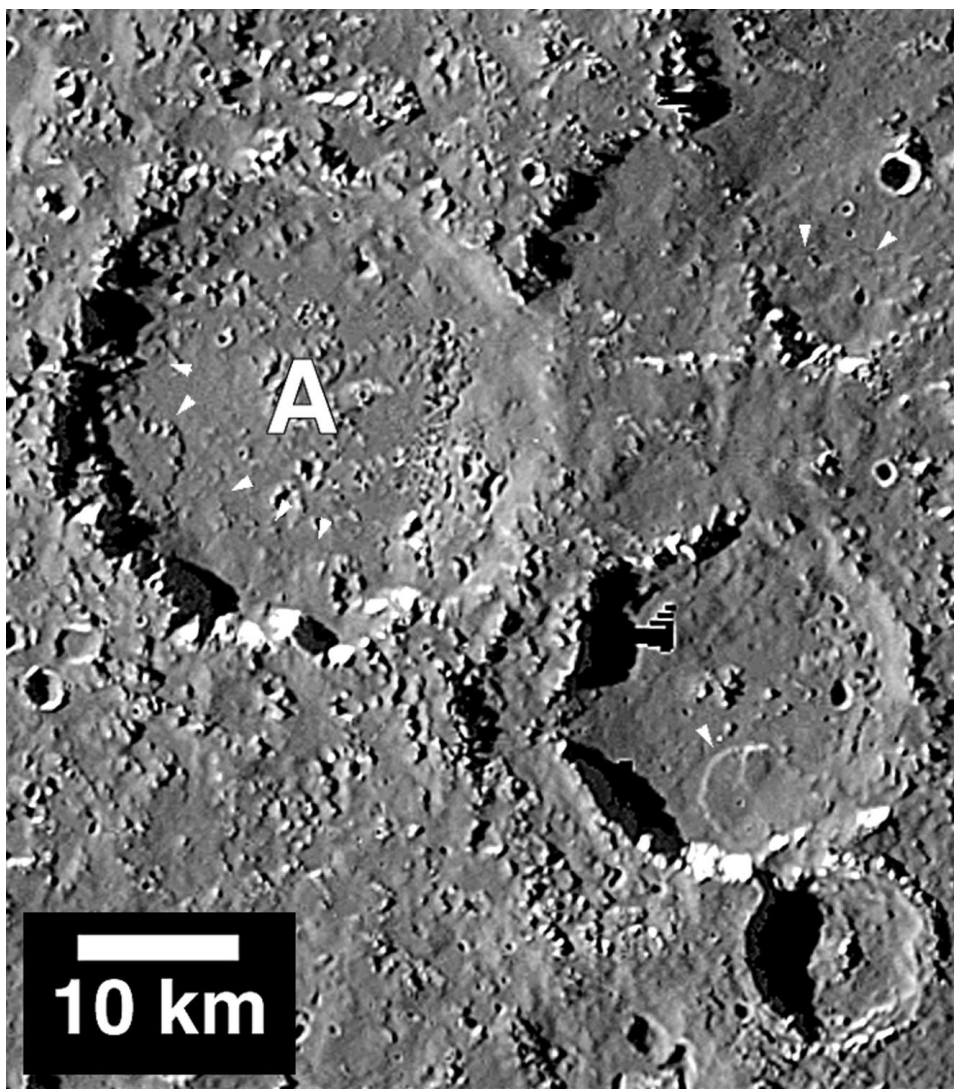


FIG. 12. Possible evidence of crater widening by multiple debris avalanches on Callisto (see arrows within crater A). Image resolution 160 m/pixel, North is up and illumination is low and from the west. Scene center coordinates are $\sim 5^{\circ}\text{S}$, 7°W . (A mosaic of portions of Galileo images PICNO C9C0005, 06, 07, 08.)

of the Valhalla region acquired during the C3 orbit. Later images show that the unit has a global extent. The near absence of small craters, which partly contributes to the visibility of the smooth unit on Callisto, may be attributable to a generally lower ratio of small-to-large impacting projectiles in the Jupiter system compared with the region of the terrestrial planets (Chapman *et al.* 1998). On the other hand, morphological descriptions of the unit (especially the spectrum of morphologies of small craters) demonstrates that there is, or has been until comparatively recently in Callisto's cratering history, an ongoing process of small-crater degradation within the smooth unit that seems to be necessarily connected to the deposition or creation of the unit. Whereas basins and large craters form rarely and would (and do) show evidence of episodic modification of Callisto's surface, small-scale impact processes act continuously, as exemplified by lunar regolith processes. Impacts serve

both to erode craters and to cover them by redistribution of ejecta. Especially if the size distribution of the impactors is characterized by a large (negative) power-law exponent, the resulting erosion and redistribution can manifest itself as a pervasive, continuous process that "softens" topographic features, as is well illustrated on the lunar surface at spatial scales smaller than a few hundred meters (e.g., Soderblom 1970, Chapman *et al.* 1996).

Such lunar-like processes are manifestly not at work on Callisto, since there is no "saturation equilibrium" population of impact craters visible on the surface. By saturation, we do not mean geometrically saturated, but rather a spatial density of small craters that is in equilibrium against the degradation and destruction of craters by the impact process alone. From experiments (Gault 1970) and direct observation of planetary surfaces, the nature of saturation equilibrium is well understood (e.g., Chapman and McKinnon 1986). For shallow-sloped power-law

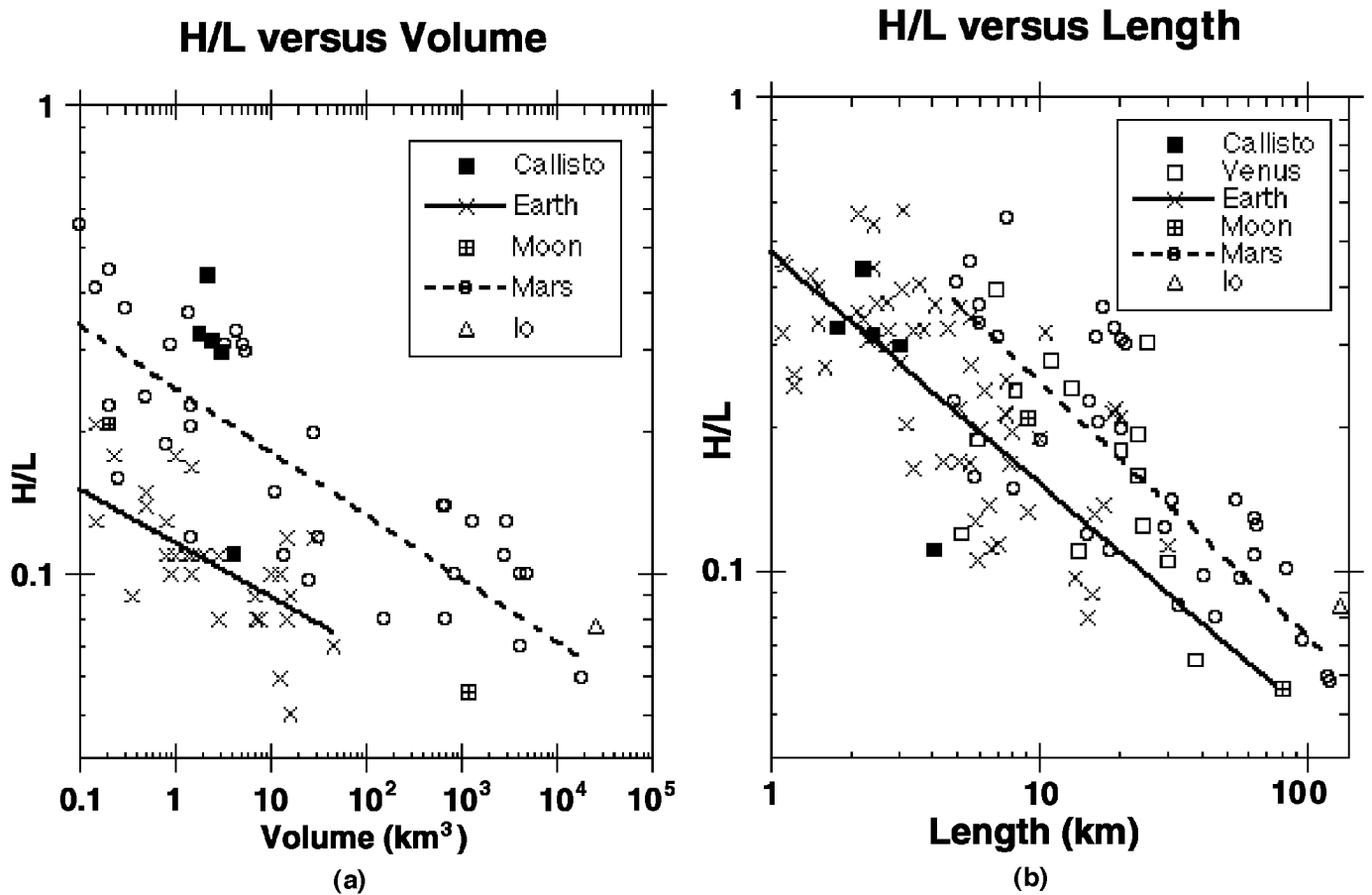


FIG. 13. Plots of Callistan debris aprons height over length ratios (H/L) versus (a) volume and (b) runout length, along with a field of measurements for similar mass movements on other objects. Non-Callistan data taken from Bulmer (1994), Schenk and Bulmer (1998), and Malin (1992).

production functions, equilibrium densities on an R plot can be as high as a few tens of percent. But the “shallow-sloped power-law production” regime of degradation is characterized by cookie-cutter-like modification of crater-rim morphology, not by smooth erosion. Moreover, it is reasonable to assume that Callisto and the dark terrain of Ganymede should, to first order, experience the same flux of primary and secondary impactors. Yet as Fig. 8 illustrates, the density of craters on Callisto becomes increasingly underabundant with decreasing crater size relative to the dark terrain of Ganymede.

The morphology of Callisto’s smooth unit could have been shaped by small impacts only if there were a steep production function, which would effectively sandblast the surface by small projectiles, more like the case of small lunar craters. In this case, the equilibrium density of craters can be as low as 10%. But the spatial density of small craters on Callisto is much lower, around 1%. In principle, such low densities could be achieved by a sandblasting process with an even larger power-law exponent, but such steep power laws have not been identified for any equilibrium population of interplanetary debris in the Solar System, and unless such a steep slope exists, small-scale impact cratering cannot account for the smooth unit on Callisto. Since Callisto is

heavily cratered by larger craters (tens of kilometers in diameter and larger) we might ask if widespread, high-velocity ejecta from those craters could emplace the smooth unit. Here, we can again look to the Moon as an analogy, because it has about the same gravity as Callisto and its highlands (large) crater populations also resemble Callisto’s. The fact that the smooth units on Callisto are so much more prominent than on the Moon immediately rules out this explanation. The maintenance of rather sharp albedo boundaries between the lunar highlands and maria, despite the nonnegligible postmare cratering of the lunar surface, illustrates the general limitations of impact processes in redistributing surface materials. In conclusion, some other process besides impact-generated and redistributed regolith probably is responsible for the appearance of craters and the smooth intercrater plains of Callisto.

Sublimation Degradation

Sublimation degradation has been proposed as an agent of kilometer-scale landform modification on several galilean satellites (McCauley *et al.* 1979, Moore *et al.* 1996). Sublimation processes relevant to (noncomet) icy bodies have been modeled

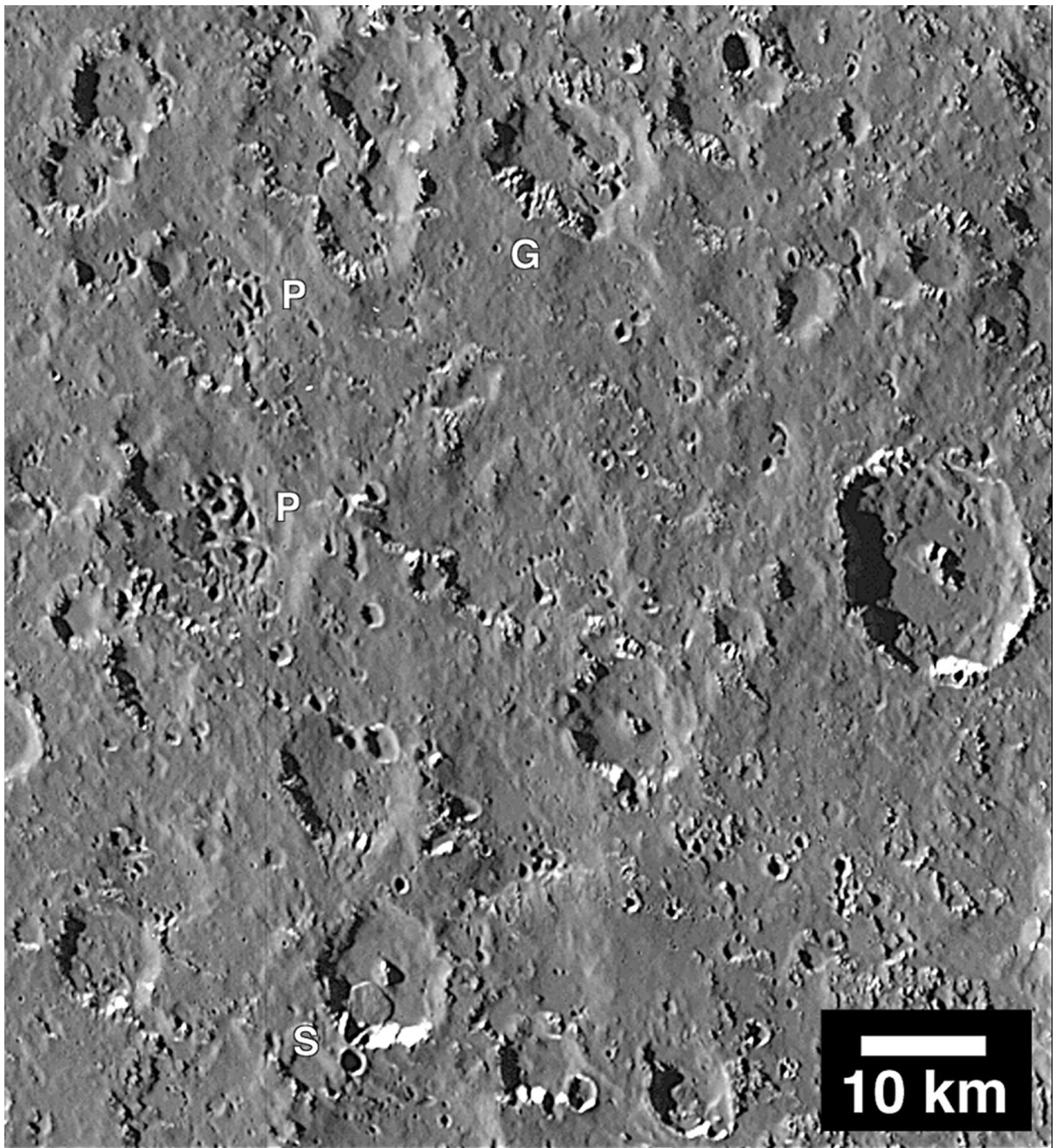


FIG. 14. Irregularly shaped pits (see near P), "gullies" (see near G), and a debris apron (see near S) all observed in this 160 m/pixel resolution image of equatorial Callisto. North is up and illumination is low and from the west. Scene center coordinates are $\sim 6^{\circ}\text{S}$, 7.5°W . (A portion of Galileo image PICNO C9C0007.)

by a number of researchers (Lebofsky 1975, Purves and Pilcher 1980, Squyres 1980, Spencer 1987a, Colwell *et al.* 1990, Moore *et al.* 1996). Purves and Pilcher (1989) and Squyres (1980) both concluded that Ganymede and Callisto should accumulate frost at their poles at the expense of the equatorial regions where exposed ice should entirely sublimate away. Spencer (1987a) modeled the thermal segregation of H_2O ice on Ganymede and Callisto and concluded that sublimation is the most significant process for the redistribution of ice at subkilometer scales.

Concepts on redistribution of surface materials by sublimation developed on the basis of Voyager data by Spencer (1987a) have been applied to much higher resolution Galileo images of Ganymede by Prockter *et al.* (1998b). These workers noted that pole-facing slopes in Galileo Regio were brighter than the opposite slopes, and they concluded that the brightening agent was a thin frost veneer, as it had no effect on underlying crater morphology. They surmised that the north/south-facing slope dichotomy in surficial frost distribution was due to sublimation

of ices on the sunnier, warmer equator-facing slopes and precipitation of frost on the less sunny (hence colder) pole-facing slopes, consistent with the hypothesis of Spencer (1987a). As ices sublime, the low albedo component of the surface materials remains behind to form a refractory-rich sublimation lag deposit. The lag may eventually become thick enough to suppress any further sublimation from underneath. Prockter *et al.* (1998b) conclude that sublimation is the primary process responsible for the albedo heterogeneity of dark terrain of Galileo Regio at small scales, and it may aid in mass wasting, but they thought that it did not contribute significantly to the degradation of large-scale morphology at that location.

Topographic thermal models for airless bodies have been constructed by several workers (e.g., Winter and Krupp 1971, Spencer 1990, Colwell *et al.* 1990). These models consider scattering and reradiation of reflected and thermal radiation from various topographic elements, and some also include diurnal subsurface heating variations. These models show that, as would be expected, poleward-facing slopes at high latitudes are cooler than the average surface and are natural sites for accumulation of frost deposits (Spencer and Maloney 1984). They also show that at low latitudes, temperatures tend to be higher in depressions, because surfaces in depressions receive thermal and reflected solar radiation from their surroundings. Low-latitude depressions, therefore, are expected to be sites of net sublimation and should develop a lag deposit on an initially icy surface somewhat faster than the plains surfaces of the same albedo. The presence of bright, icy interior crater walls at low latitudes, as is commonly seen on Callisto, therefore requires additional explanation. A possibility is that lag deposits are sloughed off these steep slopes by gravity, exposing dark dirty-ice bedrock with high thermal inertia, so that the exposed outcrop acts as a cold trap (which becomes even colder once a layer of frost forms) relative to nearby lag-covered, dark regions low thermal inertia.

The other preferred site for bright deposits at low latitudes is on the sides and summits of the numerous isolated knobs that rise out of the dark materials. Sloughing off of lag deposits and refrosting of the bedrock might explain the brightness of the slopes of these knobs, but the brightness of their summits is problematic, and the craggy, eroded appearance of these knobs must also be accounted for. Quantitative modeling of temperatures on positive relief features is more difficult than modeling crater temperatures, because crater interior temperatures are influenced only by other parts of the crater, while hill temperatures are influenced by, and influence, a wide area of the surrounding landscape. However, the following semiquantitative model yields some valuable insights.

We consider a vertical (~100-m-scale) icy scarp on Callisto at midday, overlooking a horizontal plain covered in dark material, and compare its energy balance to that of a hypothesized horizontal bright icy surface at the top of the scarp. We do not actually envision vertical cliffs. Instead, our model is a simplified one, designed to give some quantitative evaluation of scarp retreat without resorting to a complex numerical treatment. Figure 15

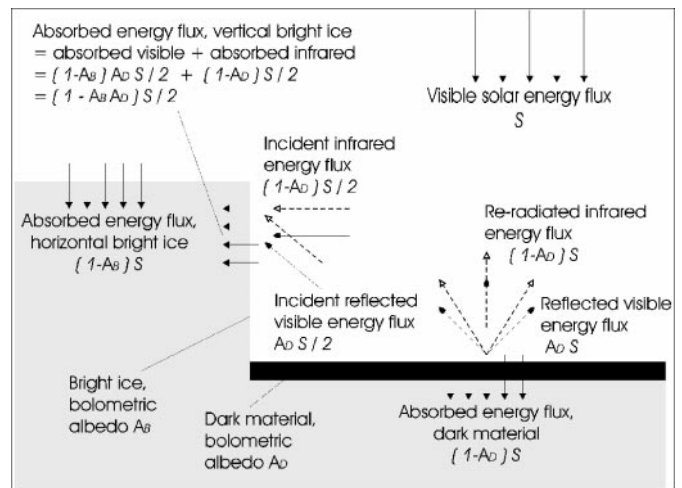


FIG. 15. Energy flux diagram. We consider a vertical icy scarp at midday, overlooking a horizontal plain covered in dark material, and compare its energy balance to that of a hypothesized horizontal bright icy surface at the top of the scarp. We assume unit emissivity for all surfaces, Lambertian scattering of sunlight, isotropic emission of thermal radiation, and negligible thermal inertia for the dark material. See text for discussion.

illustrates our model. We assume unit emissivity for all surfaces, Lambertian scattering of sunlight, isotropic emission of thermal radiation, and negligible thermal inertia for the dark material, so that absorbed solar radiation is immediately reradiated in the infrared. This last assumption is justified to first order by remote thermal measurements that show that noontime temperatures on Callisto are close to equilibrium values. We also ignore warming of the dark material by radiation from the scarp (though this is considered qualitatively later) and do not consider times other than midday.

With these assumptions, the upward energy flux from Callisto's dark material at midday is equal to the incident solar flux. Unlike the incident radiation, however, the energy is radiated isotropically, and a fraction $(1 - A_D)$ of the energy, where A_D is the bolometric albedo of the dark material, has been converted from visible and near-infrared radiation (which we call "visible" for simplicity) to thermal infrared radiation. As seen from the vertical scarp of ice, the dark material, which radiates into 2π steradians, subtends a solid angle of π steradians, so on the assumption of isotropic radiation from the dark surface, the incident visible and thermal energy flux onto the scarp is half that reflected and radiated from the dark surface, and the total is half the incident solar flux. The vertical surface, at midday, receives no direct insolation.

Because the horizontal top of the ice block receives the full incident solar flux, it would seem that it would be warmer than the vertical face, which receives only half that flux. However, ice is a good reflector of visible radiation, but a good absorber of thermal infrared radiation (e.g., Warren 1984). The assumption of unit emissivity for the ice implies that it absorbs all the incident infrared radiation that it receives from the dark material, while it will only absorb a fraction $(1 - A_B)$ of the visible

radiation, where A_b is the ice bolometric albedo. From Fig. 15, the result is that the energy flux absorbed by the vertical face is $(1 - A_b \times A_d) \times S/2$, while the horizontal ice surface absorbs $(1 - A_b) \times S$. Putting in $A_d = 0.15$ and $A_b = 0.7$, the vertical face absorbs almost 50% more energy than the horizontal face. If the thermal inertia is similar on the vertical and horizontal ice surfaces, the vertical face will therefore be warmer than the horizontal and will have a higher sublimation rate at noon. Because of the extreme temperature dependence of sublimation rates, most sublimation occurs near the peak temperature, so it is likely that diurnally averaged sublimation rates are also highest on the vertical ice surface. For a surface with many such ice scarps, there will be a net transfer of ice from the vertical scarps to nearby horizontal surfaces, and the scarps will retreat.

An additional process, not considered in the simple model above, will tend to maintain the steepness of the ice slopes. Some trapping of heat in the concave regions at the base of a slope is expected, because as in a crater interior, surfaces here see a large solid angle of surface that can radiate to them and a relatively small solid angle of deep space. The dark material at the base of the scarp will thus tend to be warmer than the dark material farther away and in turn will preferentially warm the ice near the base of the scarp. Enhanced sublimation at the scarp base will tend to maintain the steepness of the scarp as it retreats. The steepness of the scarp will prevent accumulation of a lag deposit on it: dark material released from the ice will accumulate at the base of the slope and be left behind as the scarp continues to retreat. This process provides a natural mechanism for the icy brightening of topographic crests that are so conspicuous on Callisto: scarps of exposed ice-rich bedrock will tend to retreat, with the liberated H_2O accumulating as frost on nearby horizontal surfaces and the lag accumulating at the bases of the scarps. Ice sublimates from the face of the scarp and accumulates on the top, until oversteepening causes mass wasting which exposes fresh bedrock (Fig. 16).

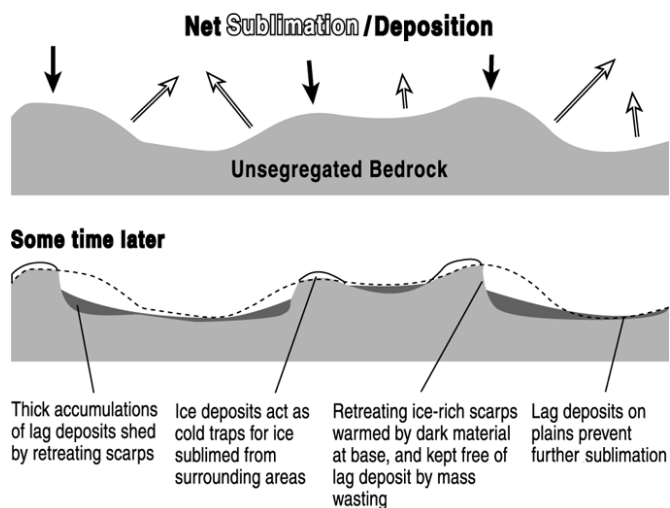


FIG. 16. Net volatile sublimation/deposition surface evolution diagram. See text for discussion.

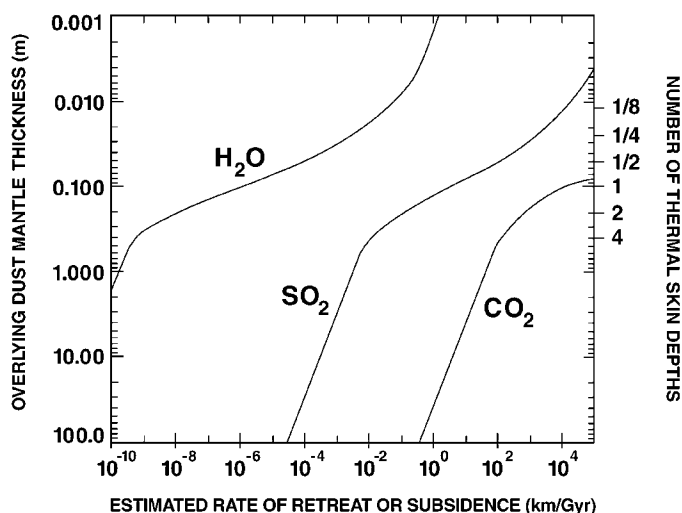


FIG. 17. Sublimation rates of different volatiles on Callisto as a function of overlying lag thickness. The lag is modeled as a fine-grain, low thermal inertia particulate. See text for discussion.

Rates of scarp retreat and ground lowering are critically dependent on the albedo and thermal inertia of the exposed surface, the depth through any lag to the icy bedrock, and the thermal inertia of that lag. These values are impossible to determine precisely; however, we can apply a simple analysis to evaluate this issue. Moore *et al.* (1996) used an application of Frick's law to evaluate the rate of sublimation for various volatiles through an overlying mantle (or lag) of very fine, loose, volatile-depleted material. Here we add the effect of a diurnal variation through a mantling material of very low thermal inertia (Fig. 17). In these model results shown in Fig. 17, we have considered the specific case of Callisto. This satellite has an ~ 400.5 -h-long diurnal cycle. Its equatorial regions experience surface temperatures in excess of 165 K and a predawn minima of ~ 80 K. The dominant low-albedo surface material is thought to be very fine (micrometer scale) and have a very low thermal inertia ($< 5 \times 10^4 \text{ erg cm}^{-2} \text{ s}^{-0.5} \text{ K}^{-1}$). In Fig. 17 we model the sublimation rate of the volatiles, selected on the bases of their detection in NIMS (near-infrared mapping spectrometer) data (McCord *et al.* 1997, 1998), buried under the dark fine material and experiencing equatorial temperatures. The dark material has a thermal skin depth of ~ 10 cm, and at four skin depths the diurnal temperatures are not varying by more than ~ 1 K (at ~ 110 K). As can be seen in Fig. 17, SO_2 and even H_2O will sublimate at rates sufficient to visibly alter landforms at SSI resolutions if these ices are very close to "hot" dust. However, a dust cover of a few tens of centimeters is sufficient to suppress the sublimation of all candidate volatiles except CO_2 . The widespread degradation of the landforms of Callisto implies that CO_2 is a significant component (a few tens of a percent) of the relief-supporting ices in the upper crust. The discovery of a tenuous CO_2 atmosphere above Callisto (Carlson 1999) lends support to this conclusion.

Large debris avalanches are more common on Callisto than on any other icy Galilean satellite, implying that the upper crust is more susceptible to sublimation-induced mechanical weakening, undermining, and undercutting than that of the other icy Galilean satellites. Landforms which may be degraded in a similar manner on Ganymede, such as the intermediate-albedo plateau material in Nicholson Regio, appear to be much less common than on Callisto where imaged by Galileo. Despite this observational limitation, we speculate that a mechanism of scarp retreat may operate at a few localities on Ganymede in which a volatile-containing plateau-forming deposit is undercut by warm material at the base of the scarp, induced by sublimation of material in the lower scarp walls. The apparent rarity of large-scale sublimation-driven landform modification on Ganymede relative to Callisto may be the consequence of fewer near-surface deposits containing substantial CO₂. Some CO₂ does appear to be present on Ganymede (McCord *et al.* 1997, 1998). The two examples discussed under Observations and Interpretations (the intermediate-albedo smooth deposits in Nicholson Regio and Xibalba Sulcus) are relatively recent (i.e., they are stratigraphically high) and, we speculate, may be of cryovolcanic origin. If so, Ganymedian deposits containing significant CO₂ may be limited to what may be the uncommon instance of postprimordial eruptions of material from volatile-rich reservoirs.

CONCLUSIONS

1. Callisto displays, by far, the most degraded surface of the icy Galilean satellites, with mass movements that are larger and apparently more common than seen elsewhere. Most degradation on Ganymede appears consistent with “dry” sliding or slumping, simple impact erosion, and regolith evolution. Dry sliding or slumping is also observed at very small (100-m-scale) scale on Europa.

2. Sputter ablation, while probably playing some role in the evolution of Ganymede’s and Callisto’s debris layers, appears to have its contribution overwhelmed by other degradational processes. Sputter ablation could potentially play a significant role on Europa only if that satellite’s surface is significantly older than 10⁸ years, which inferences from crater statistics indicate is not the case.

3. Impact erosion and regolith formation on Europa are probably minimal as implied by the low density of craters. Impact erosion and regolith formation may be largely responsible for the formation of debris and debris movements on the dark terrains of Ganymede. While impact erosion and regolith formation must operate with similar vigor on Callisto, the appearance of that satellite’s surface indicates that some other process is dominating the evolution of its surface layer.

4. Callisto, and to a lesser extent Ganymede, shows evidence for sublimation-driven landform modification and mass wasting. The extent of surface degradation implies the presence of an ice more volatile than H₂O. A candidate volatile is CO₂, which has been inferred to be present from analysis of Galileo NIMS data.

ACKNOWLEDGMENTS

We thank Eileen Ryan and an anonymous reviewer for their careful reviews of this paper. We are very appreciative of Mark Bulmer, Bernd Giese, Randy Kirk, Pascal Lee, Mike Mellon, Bob Pappalardo, Louise Prockter, Ip Wing, and Aileen Yingst for sharing their work, thoughts, and conversation, all of which greatly improved the quality of this study. This investigation was funded by NASA’s Galileo Project.

REFERENCES

- Asphaug, E., J. M. Moore, D. Morrison, P. H. Figueredo, R. Greeley, R. T. Pappalardo, L. M. Prockter, R. Tufts, and the Galileo SSI Team 1998. Crater-controlled fracture networks and the depth of ice lithospheres. In *Lunar and Planetary Science XXIX*, Abstract 1587 (CD-ROM).
- Brunsdon, D. 1979. Mass movements. In *Progress in Geomorphology* (C. E. Embleton and J. B. Thornes, Eds.), pp. 130–186. Arnold, UK.
- Bulmer, M. H. 1994. *An Examination of Small Volcanoes in the Plains of Venus, with Particular Reference to the Evolution of Domes*, Ph.D. thesis. Univ. of London, Senate House, England.
- Bulmer, M. H., and J. E. Guest 1996. Modified volcanic domes and associated debris aprons on Venus. In *Volcano Instability on the Earth and Other Planets* (W. J. McGuire, A. P. Jones, and J. Neuberg, Eds.), pp. 349–371. Geological Society Special Publication No. 110, UK.
- Carlson, R. W. 1999. A tenuous carbon dioxide atmosphere on Jupiter’s moon Callisto. *Science* **283**, 820–821.
- Chapman, C. R., and W. B. McKinnon 1986. Cratering of planetary satellites. In *Satellites* (J. A. Burns and M. S. Matthews, Eds.), pp. 492–580. Univ. of Arizona Press, Tucson.
- Chapman, C. R., W. J. Merline, B. Bierhaus, S. Brooks, and the Galileo Imaging Team 1998. Cratering in the jovian system: Intersatellite comparisons. In *Lunar and Planetary Science XXIX*, Abstract 1927 (CD-ROM).
- Chapman, C. R., J. Veverka, M. J. S. Belton, G. Neukum, and D. Morrison 1996. Cratering on Gaspra. *Icarus* **120**, 231–245.
- Chang, F. C., R. Greeley, J. E. Klemaszewski, J. M. Moore, and the Galileo SSI Team 1998. Intracrater landslides on Callisto: Observations from the Galileo nominal mission. In *Lunar and Planetary Science XXIX*, Abstract 1331 (CD-ROM).
- Coates, D. R. 1977. Landslide perspectives. *Rev. Eng. Geol.* **3**, 3–28.
- Colwell, J. E., B. M. Jakosky, B. J. Sandor, and S. A. Stern 1990. Evolution of topography on comets. II. Icy craters and trenches. *Icarus* **85**, 205–215.
- Denk, T., G. Neukum, T. B. McCord, P. D. Martin, B. E. Clark, J. W. Head, C. A. Hibbitts, G. B. Hansen, and the Galileo SSI Team 1998. Galileo-SSI color observations of the icy Galilean satellites (abs.). In *The Jovian System after Galileo, The Saturnian System before Cassini-Huygens*. International Symposium Abstracts, p. 49. Nantes, France.
- Gault, D. E. 1970. Saturation and equilibrium conditions for the impact cratering on the lunar surface: Criteria and implications. *Radio Sci.* **5**, 273–291.
- Golombek, M. P., and W. B. Banerdt 1990. Constraints on the subsurface structure of Europa. *Icarus* **83**, 441–452.
- Ip, W.-H., D. J. Williams, R. W. McEntire, and B. H. Mauk 1998. Ion sputtering and surface erosion at Europa. *Geophys. Res. Lett.*, **25**, 829–832.
- Johnson, R. E. 1990. *Energetic Charged-Particle Interactions with Atmospheres and Surfaces*. (L. J. Lanzerotti, M. Hill, and D. Stoffer, Eds.). Springer-Verlag, Berlin/Heidelberg.
- Kadel, S. D., S. A. Fagents, R. Greeley, and the Galileo SSI Team 1998. Trough-bounding ridge pairs on Europa—Considerations for an endogenic model of formation. In *Lunar and Planetary Science XXIX*, Abstract 1078 (CD-ROM).
- Kivelson, M. G., K. K. Khurana, C. T. Russell, R. J. Walker, J. Warnecke, F. V. Coroniti, C. Polanskey, D. J. Southwood, and G. Schubert 1996. Discovery of Ganymede’s magnetic field by the Galileo spacecraft. *Nature* **384**, 537–541.

- Lebofsky, L. A. 1975. Stability of frosts in the Solar System. *Icarus* **25**, 205–217.
- Malin, M. C. 1992. Mass movements on Venus: Preliminary results from Magellan cycle 1 observations. *J. Geophys. Res.* **97**, 16337–16352.
- Malin, M. C., and D. Dzurisin 1977. Landform degradation on Mercury, the Moon, and Mars: Evidence from crater depth/diameter relationships. *J. Geophys. Res.* **82**, 376–388.
- Malin, M. C., and D. C. Pieri 1986. Europa. In *Satellites* (J. A. Burns and M. S. Matthews, Eds.), pp. 689–717. Univ. of Arizona Press, Tucson.
- McCauley, J. F., B. A. Smith, and L. A. Soderblom 1979. Erosional scarps on Io. *Nature* **280**, 736–738.
- McCord, T. B., R. W. Carlson, W. D. Smythe, G. B. Hansen, R. N. Clark, C. A. Hibbitts, F. P. Fanale, J. C. Granahan, M. Segura, D. L. Matson, T. V. Johnson, and P. D. Martin 1997. Organics and other molecules in the surfaces of Callisto and Ganymede. *Science* **278**, 271–275.
- McCord, T. B., G. B. Hansen, R. N. Clark, P. D. Martin, C. A. Hibbitts, F. P. Fanale, J. C. Granahan, M. Segura, D. L. Matson, T. V. Johnson, R. W. Carlson, W. D. Smythe, G. E. Danielson, and the NIMS Team 1998. Non-water-ice constituents in the surface material of the icy Galilean satellites from the Galileo near-infrared mapping spectrometer investigation. *J. Geophys. Res.* **103**, 8603–8626.
- McEwen, A. S. 1989. Mobility of large rock avalanches: Evidence from Valles Marineris, Mars. *Geology* **17**, 1111–1114.
- McKinnon, W. B., and E. M. Parmentier 1986. Ganymede and Callisto. In *Satellites* (J. A. Burns and M. S. Matthews, Eds.), pp. 718–763. Univ. of Arizona Press, Tucson.
- Merline, W. J., C. R. Chapman, B. Bierhaus, S. Brooks, J. Moore, J. E. Klemaszewski, R. Greeley, and the Galileo Imaging Team 1998. Cratering on Callisto from the Galileo prime mission. *Bull. Am. Astron. Soc.* **30**, 1122.
- Moore, J. M., M. T. Mellon, and A. P. Zent 1996. Mass wasting and ground collapse in terrains of volatile-rich deposits as a Solar System-wide geological process: The pre-Galileo view. *Icarus* **122**, 63–78.
- Pappalardo, R. T., J. W. Head, G. C. Collins, R. L. Kirk, G. Neukum, J. Oberst, B. Giese, R. Greeley, C. R. Chapman, P. Helfenstein, J. M. Moore, A. McEwen, B. R. Tufts, D. A. Senske, H. H. Breneman, and K. Klaasen 1998a. Grooved terrain on Ganymede: First results from Galileo high-resolution imaging. *Icarus* **135**, 276–302.
- Pappalardo, R. T., J. W. Head, R. Greeley, R. J. Sullivan, C. Pilcher, G. Schubert, W. B. Moore, M. H. Carr, J. M. Moore, M. J. S. Belton, and D. L. Goldsby 1998b. Geological evidence for solid-state convection in Europa's ice shell. *Nature* **391**, 365–367.
- Passy, Q. R., and E. M. Shoemaker 1982. Craters and basins on Ganymede and Callisto: Morphological indicators of crustal evolution. In *Satellites of Jupiter* (D. Morrison, Ed.), pp. 379–434. Univ. of Arizona Press, Tucson.
- Pike, R. J. 1980. Geometric interpretation lunar craters. *U.S. Geol. Surv. Prof. Paper* **1046**, C1-C77.
- Prockter, L. M., J. W. Head, R. T. Pappalardo, E. Asphaug, and the Galileo SSI Team 1998a. Geology of Nicholson regio from Galileo imaging: Evidence for tectonic focusing through craters. In *Lunar and Planetary Science XXIX*, Abstract 1336 (CD-ROM).
- Prockter, L. M., J. W. Head, D. A. Senske, R. T. Pappalardo, G. Neukum, R. Wagner, U. Wolf, J. Oberst, B. Giese, J. M. Moore, C. R. Chapman, P. Helfenstein, R. Greeley, H. H. Breneman, and M. J. S. Belton 1998b. Dark terrain on Ganymede: Geological mapping and interpretation of Galileo Regio at high resolution. *Icarus* **135**, 317–344.
- Purves, N. G., and C. B. Pilcher 1980. Thermal migration of water on the Galilean satellites. *Icarus* **43**, 51–55.
- Schenk, P. M., and M. H. Bulmer 1998. Origin of mountains on Io by thrust faulting and large-scale mass movements. *Science* **279**, 1514–1517.
- Schenk, P. M., and W. B. McKinnon 1989. Fault offsets and lateral crustal movement on Europa: Evidence for a mobile ice shell. *Icarus* **79**, 75–100.
- Sharp, R. P. 1973a. Mars: South polar pits and etched terrain. *J. Geophys. Res.* **78**, 4222–4230.
- Sharp, R. P. 1973b. Mars: Fretted and chaotic terrains. *J. Geophys. Res.* **78**, 4073–4083.
- Sharpe, C. F. S. 1939. *Landslides and Related Phenomena*. Cooper Square, New York.
- Shoemaker, E. M., and E. C. Morris 1969. Thickness of the regolith. In *Surveyor Project Final Report. II. Science Results*, pp. 102–104, JPL Tech Report 32-1265. Jet Propulsion Laboratory, Pasadena.
- Shoemaker, E. M., B. K. Lucchitta, J. B. Plescia, S. W. Squyres, and D. E. Wilhelms 1982. The geology of Ganymede. In *Satellites of Jupiter* (D. Morrison, Ed.), pp. 435–520. Univ. of Arizona Press, Tucson.
- Soderblom, L. A. 1970. A model for small-impact erosion applied to the lunar surface. *J. Geophys. Res.* **75**, 2655–2661.
- Spencer, J. R. 1987a. Thermal segregation of water ice on the Galilean satellites. *Icarus* **69**, 297–313.
- Spencer, J. R. 1987b. *The Surfaces of Europa, Ganymede, and Callisto: An Investigation Using Voyager IRIS Thermal Infrared Spectra*, Ph.D. dissertation. Univ. of Arizona Press, Tucson.
- Spencer, J. R. 1990. A rough-surface thermophysical model for airless planets. *Icarus* **83**, 27–38.
- Spencer, J. R., and P. R. Maloney 1984. Mobility of water ice on Callisto: Evidence and implications. *Geophys. Res. Lett.* **11**, 1223–1226.
- Squyres, S. W. 1980. Surface temperatures and retention of H₂O frost on Ganymede and Callisto. *Icarus* **44**, 472–480.
- Varnes, D. J. 1958. Landslide types and processes. In *Landslides and Engineering Practice* (E. B. Eckel, Ed.), pp. 20–47. Nat. Acad. Sci., National Research Council Highway Research Board, Washington, DC.
- Varnes, D. J. 1978. Slope movement types and processes. In *Landslide, Analysis, and Control* (R. L. Shuster and R. J. Kriszek, Eds.), pp. 11–33. Nat. Acad. Sci., National Research Council Transportation Research Board, Washington, DC.
- Warren, S. J. 1984. Optical constants of ice from the ultraviolet to the microwave. *Appl. Optics* **23**, 1206–1225.
- Winter, D. F., and J. A. Krupp 1971. Directional characteristics of infrared emission from the Moon. *Moon* **2**, 279–292.
- Yingst, R. A., J. W. Head, J. M. Moore, C. R. Chapman, R. Pappalardo, and the Galileo Imaging Team 1997. Ganymede bright terrain at very high resolution: Geologic structure and regolith processes. In *Lunar and Planetary Science XXVIII*, pp. 1611–1612.
- Yingst, R. A., J. W. Head, R. T. Pappalardo, C. R. Chapman, J. M. Moore, and the Galileo SSI Team 1998. Geologic structure and regolith processes of Xibalba Sulcus, Ganymede as indicated by very high resolution Galileo imagery. In *Lunar and Planetary Science XXIX*, Abstract 1318 (CD-ROM).
- Zahnle, K., H. Levison, and L. Dones 1998. Cratering rates on the Galilean satellites. *Icarus* **136**, 202–222.